BER Performance Improvement in UWA Communication via Spatial Diversity

Snigdha Bhuyan

Department of Electronics and Communication Engineering
National Institute of Technology Rourkela

BER Performance Improvement in UWA Communication via Spatial Diversity

Thesis submitted in partial fulfillment

of the requirements of the degree of

Master of Technology

in

Electronics and Communication Engineering
(*Specialization*: *Communication and Networks*)

by

Snigdha Bhuyan

(Roll Number: 214EC5409)

based on research carried out

under the supervision of

Asst.Prof. Dr.Siddharth Deshmukh

May, 2016

Department of Electronics and Communication Engineering
National Institute of Technology Rourkela

Department of Electronics and Communication Engineering
National Institute of Technology Rourkela

May 30, 2016

Certificate of Examination

Roll Number: *214EC5409*
Name: *Snigdha Bhuyan*
Title of Dissertation: *BER Performance Improvement in UWA Communication via Spatial Diversity*

We the below signed, after checking the dissertation mentioned above and the official record book (s) of the student, hereby state our approval of the dissertation submitted in partial fulfillment of the requirements of the degree of *Master of Technology* in *Electronics and Communication Engineering* at *National Institute of Technology Rourkela*. We are satisfied with the volume, quality, correctness, and originality of the work.

Dr.Siddharth Deshmukh
Principal Supervisor

Department of Electronics and Communication Engineering
National Institute of Technology Rourkela

Asst.Prof. Dr.Siddharth Deshmukh
Assistant Professor

May 30, 2016

Supervisor's Certificate

This is to certify that the work presented in the dissertation entitled *BER Performance Improvement in UWA Communication via Spatial Diversity* submitted by *Snigdha Bhuyan*, Roll Number 214EC5409, is a record of original research carried out by her under my supervision and guidance in partial fulfillment of the requirements of the degree of *Master of Technology* in *Electronics and Communication Engineering*. Neither this thesis nor any part of it has been submitted earlier for any degree or diploma to any institute or university in India or abroad.

Dr.Siddharth Deshmukh

Dedicated to My Family,Guide and Friends...

Declaration of Originality

I, ***Snigdha Bhuyan***, Roll Number ***214EC5409*** hereby declare that this dissertation entitled ***BER Performance Improvement in UWA Communication via Spatial Diversity*** presents my original work carried out as a postgraduate student of NIT Rourkela and, to the best of my knowledge, contains no material previously published or written by another person, nor any material presented by me for the award of any degree or diploma of NIT Rourkela or any other institution. Any contribution made to this research by others, with whom I have worked at NIT Rourkela or elsewhere, is explicitly acknowledged in the dissertation. Works of other authors cited in this dissertation have been duly acknowledged under the sections "Reference" or "Bibliography". I have also submitted my original research records to the scrutiny committee for evaluation of my dissertation.

I am fully aware that in case of any non-compliance detected in future, the Senate of NIT Rourkela may withdraw the degree awarded to me on the basis of the present dissertation.

May 30, 2016
NIT Rourkela

Snigdha Bhuyan

Acknowledgment

I would like to express my gratitude to my guide **Dr. Siddharth Deshmukh** for his guidance, advice and invaluable support throughout my research work. I am especially indebted to him for always motivating me to do new things, enlighten me with both research and writing skills. Without his knowledge, divergent thinking, patience and enthusiasm to answer any question this research would have never been possible.It has been a great honour and pleasure for me to do research under supervision of Prof. Siddharth Deshmukh. Working with him has been a great experience. I would like to thank him for being my mentor here at National Institute of Technology, Rourkela.

I am also thankful to **Prof.K.K. Mahaptra**, **Prof.S.K. Patra**, **Prof.S.K. Behera**, **Prof.S. Meher**, **Asst.Prof.D.P. Acharya**, **Asst.Prof.S.K. Das**, **Asst.Prof.S.M. Heramath**, **Asst.Prof.A.K. Sahoo**, **Prof.S. Maiti**, **Prof.A.K. Swain**, **Asst.Prof.L.P. Roy** for giving me knowledge. They have been great sources of inspiration to me and I thank them from the bottom of my heart. I would like to thank to all my faculty members and staff of the Department of Electronics and Communication Engineering, N.I.T. Rourkela, for their generous help for their cooperation during the tenure spent here.

I would like to express my sincere thanks to Mrs.Jaspreet Bhatia, Ms.Ayaskanta Pandia, Mr.Rajesh Nayak for always motivating me and making me realize my potential.I am thankful to thank all my classmates, seniors for their endless support.I've enjoyed their companionship so much during my stay at NIT, Rourkela.

I am especially indebted to my parents, sister and brother-in-law for their love, sacrifice, support and guidance at every step of my life.

May 30, 2016 *Snigdha Bhuyan*
NIT Rourkela Roll Number: 214EC5409

Abstract

In present era while wireless communication has become an integral part of our life, the advancements in underwater communications (UWA) is still seem farfetched. Underwater communication is typically essential because of its ability to collect information from remote undersea locations. It don't use radio signals for signal transmission as they can propagate over extremely short distance because of degradation in signal strength due to salinity of water, rather it uses acoustic waves. The underwater acoustic channel has many characteristics which makes receivers very difficult to be realized. Some of the characteristics are frequency dependent propagation loss, severe Doppler spread multipath, low speed of sound. Due to motion of transmitter and receiver the time variability and multipath makes underwater channel very difficult to be estimated. There are various channel estimation techniques to find out channel impulse response but in this thesis we have considered a flat slow fading channel modeled by Nakagami-m distribution. Noise in underwater communication channel is frequency dependent in nature as for a particular range of frequency of operation one among the various noise sources will be dominant. Here they don't necessarily follow Gaussian statistics rather follows Generalized Gaussian statistics with decaying power spectral density. The flexible parametric form of this statistics makes it useful to fit any source of underwater noise source. In this thesis we have gone through two step approach. In the first step, we have considered transmission of information in presence of noise only and designed a suboptimal maximum likelihood detector. We have compared the performance of this proposed detector with the conventional Gaussian detector where decision is taken based on a single threshold value and the threshold value is calculated by using various techniques. Here it is being observed that the ML detector outperforms the Gaussian detectors and the performance can be improved further by exploiting the multipath components. In the second step we have considered channel along with noise and have designed a ML detector where we have considered the receiver is supplied with two copies of the same transmitted signal and have gone through a two-dimensional analysis. Again we compared the performance with conventional maximal ratio combiner where we can observe the ML detector performance is better. Further we have incorporated selection combining along with these detectors and compared the performance. Simulation results shows that the proposed detector always outperforms the existing detectors in terms of error performance.

Contents

Certificate of Examination ii

Supervisor's Certificate iii

Dedicated to My Family,Guide and Friends... iv

Declaration of Originality v

Acknowledgment vi

Abstract vii

List of Figures x

List of Tables xii

1 Introduction 1

1.1 Underwater Acoustic Communication 1
1.2 Why acoustic wave? 1
1.3 Acoustic Waves 2
1.4 Literature Review 3
1.5 Research Objective) 4
1.6 Thesis Organization 4

2 UWA Noise Model 6

2.1 Underwater Acoustic Communication 6
2.2 Parameters of Noise 7
2.2.1 Mean (or) Expected value 7
2.2.2 n^{th} moment 7
2.2.3 Kurtosis 7
2.3 Noise Distribution in UWA communication 8
2.4 GG Distributed Noise Sample Generation 10
2.4.1 Inverse Transform Sampling 10
2.4.2 Quantile Function of GG distribution 11

3 UWA Fading Model **13**
3.1 Preview . . . 13
3.2 Scales of Fading . . . 13
3.2.1 Large Scale Fading . . . 14
3.2.2 Small Scale Fading . . . 14
3.3 Fading Distributions . . . 15
3.3.1 Rayleigh Fading . . . 15
3.3.2 Rician Fading . . . 16
3.3.3 Nakagami-m Distribution . . . 16

4 Detector Design(without fading) **20**
4.1 Optimal Detector . . . 20
4.2 Suboptimal Detectors . . . 21
4.2.1 Gaussian/Linear Detector . . . 21
4.2.2 Sign Correlator . . . 21
4.2.3 Cauchy detector and Myriad Filter . . . 22
4.2.4 Soft Limiter . . . 22
4.2.5 Locally Optimal Bayesian Detector . . . 23
4.3 Linear Detector . . . 23
4.3.1 System Model . . . 24
4.3.2 Probability of error Calculation . . . 24
4.3.3 Simulation Results and Discussion . . . 30
4.4 Expectation Maximization Algorithm . . . 34
4.4.1 Non-structure index/Overlap index . . . 35
4.4.2 Gaussian Factor (Γ) . . . 35
4.5 Proposed Detector in Presence of Noise Only . . . 36
4.5.1 System Model . . . 36
4.5.2 Approximated ML Detector with Reduced Complexity . . . 37
4.5.3 Simulation Results and Discussion . . . 42

5 Detector Design(with fading) **46**
5.1 Approximated ML Detector with Reduced Complexity . . . 46
5.2 Simulation Results . . . 50

6 Conclusion and Future scope **54**
6.1 Conclusion . . . 54
6.2 Future Scope . . . 54

References **55**

Dissemination **57**

List of Figures

2.1 Probability density function for different kurtosis values 9
2.2 Cummulative Distribution Function for different kurtosis values 10
2.3 Normalized histogram and theoritical PDF comparision (a)$\beta = 6$ and kurtosis=2 (b)$\beta = 2$ and kurtosis=3 (c)$\beta = 1.4063$ and kurtosis=4 (d)$\beta = 1$ and kurtosis=6 12

3.1 Nakagami Probability density function 17

4.1 Decision region when receiver has two copies of the same transmitted signal 22
4.2 diagram of soft limiter 23
4.3 diagram of locally optimal bayesian detector 23
4.4 BPSK constellation diagram 25
4.5 QPSK constellation diagram 28
4.6 BER of BPSK signaling for zero mean of noise 31
4.7 BER of BPSK signaling for non-zero mean of noise 32
4.8 BER of QPSK signaling for zero mean of noise 33
4.9 BER of QPSK signaling for non-zero mean of noise 34
4.10 Approximation of GG noise for $\beta = 2 and 2.7787$ by two Gaussian components 37
4.11 Conditional distribution of received signal under Hypothesis H_0 and H_1 . . 38
4.12 Decision boundary with one receiving antenna 38
4.13 Two dimensional decision region for two copies of received signal 39
4.14 Decision boundary for second quadrant in case of two receiving antennas . 40
4.15 Complete Decision boundary with two receiving antennas 41
4.16 Complete Decision boundary with two receiving antennas 42
4.17 Detector performance comparison with single antenna reception 43
4.18 Detector performance comparison with two receiving antenna 44
4.19 Performance improvement via spatial diversity 44

5.1 Two dimensional decision regions for two copies of received signal affected by channel 47
5.2 Conditional distribution of received signal under Hypothesis H_0 and H_1 . . 48
5.3 Decision boundary for second quadrant in case of two receiving antennas . 49
5.4 Decision region in 2^{nd} quadrant for different SNR values 49

5.5 Complete decision boundary for two receiving antennas 50
5.6 Performance comparison between proposed detector and MRC detector . . 51
5.7 Performance comparison between proposed detector and MRC detector along with selection combining 52
5.8 Performance comparison of ML detector for different values of shape parameter of fading 52

List of Tables

2.1 Oceanic noise frequency spectrum 6
2.2 Shape parameter and kurtosis for different noise sources 8

3.1 Comparison of fitness of different models to empirical data for 505m . . . 18
3.2 Comparison of fitness of different models to empirical data for 200m 19

4.1 Quadrature phase shift keying bit configuration 28

Chapter 1

Introduction

1.1 Underwater Acoustic Communication

Underwater acoustic communication is a process sending and receiving information through water media. Underwater is the most complex channel in present era to be modeled and used. Acoustic communication in underwater generally is implemented using sensor nodes on sea bed and UUVs or AUVs. UWA communication is established mostly using hydrophones. It is a microphone used for recording or listening to underwater sound. Hydrophones are kind of piezoelectric transducer which generates proportionate electricity when is subjected to any pressure change.

Underwater communication has gained prolific attention by researchers because of willingness to explore underwater phenomena and their effect in order to get rid of disasters. Some of the applications are scientific data collection such as geoscience, marine biology etc, military and non-military survey such as data objects detection, sea bottom imaging etc, discovery of natural resources, marine phenomena, environmental monitoring such as pollution control, climatic information, prediction of natural disasters, gas and oil field detection and protection etc.

1.2 Why acoustic wave?

In wireless communication we prefer EM waves for transmission of data. Water is found to be insulator in its purest form but it contains dissolved salts and other matters which makes it partial conductor. Sea water has high salt content which makes it a perfect conductor with conductivity varying from average of 2mhos per meter (cold water) to 8mhos per meter (warm water). So EM waves fades rapidly in sea water and unable to cover large distance or in order to travel longer distance they need large antennas. Attenuation amount that EM waves undergoes in sea water is given as,

$$Attenuation in dB/meter = 0.0173\sqrt{f\sigma} \tag{1.1}$$

Where f: frequency of operation in Hz

σ: Conductivity in mho/meter Optical waves provides high bit rate but over short distance

only. Here information is conveyed an intercepted in the form of intensity of light. As optical wave moves water media offers high attenuation and dispersion due to which intensity of light fades rapidly and undergoes severe scattering.[1] Due to these reasons acoustic waves are best suited for underwater communication.

1.3 Acoustic Waves

Parameters of acoustic waves used for underwater communication are highly affected by sea water characteristics and frequency of operation. Speed of propagation of acoustic wave is dependent on salinity, temperature and pressure of the medium. The average speed of acoustic wave is 1500m/s (in the range of 1450m/s to 1550m/s)[2].This low speed of acoustic waves causes more time for reception of signal which makes the communication system very complicated because except transmitting useful information it also needs many handshaking signals as per communication protocols. This delay causes severe multipath interference as delay spread is more. Echoes in UWA communication span up to tens and hundreds of symbol. One way to avoid this is to insert some time gap between successive symbol transmissions which must be at least equal to the delay spread. But this causes slower data rate. As coherence bandwidth is inversely proportional to the delay spread so the channel is frequency selective in nature. Low speed of sound causes severe Doppler distortion also. When we consider a mobile environment that is both transmitter and receiver are moving if the relative velocity between them is $\pm v$, transmitter frequency is f_c then the frequency observed at the receiver is $f_c(1 \pm \frac{v}{c})$. As speed of propagation i.e. 'c' is very less so the factor v/c can take several orders of magnitude. This large Doppler spread causes less coherence time and this implies that UWA channel is highly time-varying in nature. The distance to be covered in UWA communication depends on frequency of operation. As frequency of operation increases the distance covered by acoustic wave decreases as well as the bandwidth. UWA communication is wideband in nature as both frequency of operation and bandwidth is in the order of KHz. Acoustic path loss depends on the signal frequency and distance. This dependence is because of absorption which is nothing but transfer of acoustic energy into heat. Spreading loss is another reason which refers to decrease in energy level of signal as it moves away from the source as energy spreads out. The absorption coefficient is the major limiting factor on frequency of operation as it increases with increasing frequency. The multipath propagation occurs due to many reasons as explained next. Surface duct is one of them where wave covers a larger distance by successive reflection. Surface reflection that occurs on the sea surface because of its roughness and smoothness. Another one reason is bottom bounce where wave is reflected from sea bed. The irregularity in sea water in vertical channel also causes refraction causing multipath propagation.

1.4 Literature Review

Underwater acoustic (UWA) communication has gained prolific attention in last few decades leading to development of various techniques with improved performance and robustness. Performance of these communication systems operating undersea are subjected to unique characteristics of channel. Due to huge degradation in signal strength while propagation through sea water, electromagnetic waves are not suitable rather acoustic waves are enabled for communication[3] . The applications in UWA communication include collection of oceanographic data, military surveillance, disaster prevention etc [4]. The challenges in design of suitable communication system are attributed to some of the unique characteristics of underwater medium. Digital communication through UWA medium is substantially different from other medium as it undergoes a time varying, complex and nonlinear multipath channel. The transmission loss increases with increase in frequency as well as range of operation [3],[5],[6]. Low propagation speed of acoustic waves results in large multipath delay spread and hence there is severe inter symbol interference at the receiver [7],[8]. Further, additive noise in the underwater acoustic (UWA) channel is significantly different from wireless channel. The UWA communication in oceanic medium is affected by prevailing noise sources like, surface waves, thermal noise, turbulence etc.[9] and spontaneous sources like marine life, shipping traffic, underwater explosives, offshore exploration etc. [10]. Due to dominance of different noise sources in various acoustic spectrum bands, standard Gaussian distribution is not suitable for characterization of additive noise in UWA channel. For example, in spectrum range of 1Hz to 100Hz there is dominance of seismic noise, while in range of 10Hz to 100 KHz there is dominance of noise due to merchant ships [8]. Since most communication systems are designed assuming additive white Gaussian noise (AWGN) model, in this paper we investigate a new receiver design technique to improve the communication system performance in UWA environment. The additive noise in UWA communication can be characterized by several non Gaussian models, like Middleton model, Gaussian Gaussian model, Generalized Gaussian (GG) model etc. each having its own limitations. Middleton model have infinite series of weighted Gaussian density, while Gaussian Gaussian models are not able to capture the shape and tail of actual noise distribution [11],[12]. In this work, we choose GG distribution to model UWA channel noise as by adjustment of distribution parameters, the model can be easily adapted to super Gaussian and sub Gaussian densities [13]. The UWA channel noise is modeled by GG distribution in [14] to derive the analytical expression for probability of error performance. The authors have considered BPSK, QPSK, and M-ary PAM modulation schemes and analyzed the receiver performance under various Kurtosis values. Considering simplicity in design, a linear detector which is optimal for noise with Gaussian distribution can be used[15]. However, its performance is expected to degrade as GG statistics move away from Gaussian statistics. Similarly, a sign correlator based receiver can be used; but it performs

better only if supplied with odd copies of same transmitted signal [12]. Sub-optimal linear detectors based on optimal nonlinear function can be also used, but it performs poorly at high SNR values [11]. There are various distribution which can model the randomness of channel like Rayleigh, Rician, Nakagami etc. We will choose Nakagami fading as it is a more generalized distribution which fits better to any empirical data. The flexible parametric form of Nakagami distribution with shape parameter makes it fit to less fading to severe fading condition [16] and in[17] it is observed that a Nakagami based channel model can be used to simulate the channel behavior of real data sets.

1.5 Research Objective)

The receiver designed for UWA communication considers noise to be Gaussian in nature which is actually not the case. Noise in UWA communication depends on the frequency of operation as well as the source of noise. They can't be modeled by standard normal distribution. They are modeled by generalized Gaussian distribution. This distribution is impulsive in nature and very difficult to be analyzed. So in this thesis we have decomposed the noise in terms of weighted Gaussian components. A detector designed by considering noise to be Gaussian gives poor performance if noise becomes impulsive due to some parameters. The research objective can be summarized as,

- Design of a receiver that will give desired performance independent of noise parameters. This will be designed once considering only noise which is GG distributed.
- Again we have considered channel which is Nakagami distributed along with noise and design a receiver whose performance is superior to that of existing conventional detectors.

1.6 Thesis Organization

This thesis comprises of five chapters. The background details of UWA communication, parameters acoustic wave, channel critical parameters and characterization are discussed in the current chapter. The objective of the research work is also mentioned.

- **chapter 2** includes discussion on various categories of noise existing in UWA communication. Various critical parameters related to sea noise sources are explained and a proper noise model is developed. The method of noise sample generation with appropriate distribution is mentioned.
- **chapter 3** explains various categories of fading based on some critical entities related to noise. Then several channel distributions are mentioned and the reason of opting for Nakagami fading is discussed.

- **chapter 4** models the communication system.First it will include description about the existing detectors and their limitations. Then it will explain the technique used in proposed detector where we have not considered the channel fading.
- **chapter 5** models the communication system where we have designed a detector considering the channel fading along with noise.
- **chapter 6** concludes the research work done with and future scope.

Chapter 2

UWA Noise Model

2.1 Underwater Acoustic Communication

Noise is another important factor for receiver design in UWA communication. Most of the receivers are designed by assuming that noise in UWA communication follows Gaussian statistics [14]but here noise is not white rather have a decaying power spectral density. Presence of large number of noise sources classifies them broadly into two categories as (a) prevailing (or) ambient noise (b) intermittent (or) site-specific noise [8].

(a) **Prevailing (or) Ambient noise** This category of noise is generally always present in the background especially in quiet deep sea. This includes sources like thermal noise, surface waves, surface agitation, turbulence, rain etc.

(b) **Intermittent (or) Site-specific noise**This category of noise is present in specific sites for example in polar region breakage of ice serves as noise. Earthquake, explosions, merchant ships, biological noise etc are few of the sources serving in this category.

The power spectral density degradation depends on the nature of the noise source. If for example we consider surface waves then with increasing speed of surface wave the rate of decay of PSD increases. The PSD decreases approximately at a rate of 18dB/decade [8],[1]. Noise in UWA communication is frequency dependent in nature. Among the various existing sources of noise, for a particular range of frequency of operation a particular source of noise becomes dominant in nature. For example, seismic noise dominates in the range of 1Hz to 100Hz, whereas for 10Hz to 10 KHz spectrum band noise from merchant ships is dominant in nature [14]. The dominant noise sources for different band of operation are given in table 1.1.

Table 2.1: Oceanic noise frequency spectrum

Source	**Frequency(in Hz)**	**Source**	**Frequency(in Hz)**
Merchant ships	10-10K	Turbulence,Seismic Noise	1-100
Biological Noise	10-100K	Surface Waves	100->10K
Earthquake	1-100	Surface Agitation	1-10
Explosions	1-100	Thermal Noise	10K-100K

2.2 Parameters of Noise

2.2.1 Mean (or) Expected value

The expected value of a random variable 'x' with PDF *f(x)* is defined as,

$$\mu = \mathrm{E}\left(\mathrm{x}\right) = \int_{-\infty}^{\infty} \mathrm{x}\mathrm{f}\left(\mathrm{x}\right)\mathrm{dx}$$

and signifies the statistical average of the random variable which is the first non- central moment.

2.2.2 n^{th} moment

The nth non-central moment of a random variable 'x' is defined as,

$$\mathrm{E}\left(\mathrm{x}^{\mathrm{n}}\right) = \int_{-\infty}^{\infty} \mathrm{x}^{\mathrm{n}}\mathrm{f}\left(\mathrm{x}\right)\mathrm{dx}$$

For n=2, it defines the **R.M.S. power** of the random variable. The nth central moment of a random variable 'x' is defined as,

$$\mathrm{E}\left(\mathrm{x}^{\mathrm{n}}\right) = \int_{-\infty}^{\infty} \left(\mathrm{x}-\mu\right)^{\mathrm{n}}\mathrm{f}\left(\mathrm{x}\right)\mathrm{dx}$$

It is named so because the moment is taken relative to mean. For n=2, it reduces to second central moment which is called as variance of the random variable. Variance of noise signifies the spreading of noise distribution about its mean. A higher value denotes more spreading about the mean and tells there is a significant probability that the random variable will take values away from the mean and vice versa. For zero value of mean variance becomes equal to R.M.S. power.

2.2.3 Kurtosis

Kurtosis is a special parameter which is used to define the tailedness of a random variable and is defined fourth moment as,

$$\mathrm{kurtosis} = \frac{\frac{1}{\mathrm{N}}\sum_{i=1}^{N}\left(\mathrm{x}-\mu\right)^{4}}{\left(\frac{1}{\mathrm{N}}\sum_{i=1}^{N}\left(\mathrm{x}-\mu\right)^{2}\right)^{2}}$$

This parameter plays an important is signifying whether the variable is heavy-tailed or light-tailed in relative to normal distribution. A perfect normal distribution has kurtosis value

Table 2.2: Shape parameter and kurtosis for different noise sources

Noise Source	**Shape Parameter**(β)	**Kurtosis-K[N}**
Ship transit noise	2..7787	2.5
Classical Gaussian random variable	2	3
Noise from sea surface agitation	1.62844	3.5

'3'. Excess kurtosis is defined as the difference between the obtained kurtosis value and kurtosis value of normal distribution. If excess kurtosis>0 then distribution is **leptokurtic** in nature which is tighter. They are having flat tail approaching towards zero more slowly in comparison to Gaussian distribution producing more outliers. A clear example of this category is Laplace distribution If excess kurtosis<0 then distribution is **platykurtic** in nature which is flat-topped in nature. They approach towards zero at a faster rate in comparison to Gaussian distribution producing significantly less outliers. Uniform distribution falls under this category tailedness.

2.3 Noise Distribution in UWA communication

The noise sources existing in UWA communication exhibits different distributions which can be best described by Generalized Gaussian distribution (GGD). The flexible parametric form makes very easy to fit into distribution of any noise. If 'n' represents the noise, then PDF expression is given by,

$$f_{(N-GG)}(n) = \beta/(2\alpha\Gamma(1/(\beta)))exp\{-(|n-\mu_n|/\alpha)^{\beta}\}\alpha, \beta > 0, \mu \in R, N \in R$$

Where, μ_n is the mean representing the location of the noise distribution, α is the scale parameter which represents the peak of the distribution, β is the shape parameter which is a very important parameter as is directly related to kurtosis of noise, $\Gamma()$ is the standard gamma function. The variance and kurtosis expression can be given by,

$$\sigma_{\mathrm{n}}^2 = \frac{\alpha^2 \left({}^{3}/_{\beta}\right)}{\left({}^{1}/_{\beta}\right)}$$

and

$$\mathrm{Kurt\,[N]} = \frac{\left({}^{1}/_{\beta}\right)\left({}^{5}/_{\beta}\right)}{\left({}^{3}/_{\beta}\right)^{2}}$$

GG distribution can fit into any set of empirical data proper selection of β .Table II shows values of shape parameter for different noise sources. The PDF plot GG distribution is,

In fig 2.1 as we have considered a constant value of scale parameter we can observe that the height of all the distributions for different values of shape parameter (or) kurtosis is same. For $\beta = 2$ kurtosis takes a value of 3 representing standard normal distribution. Here we can

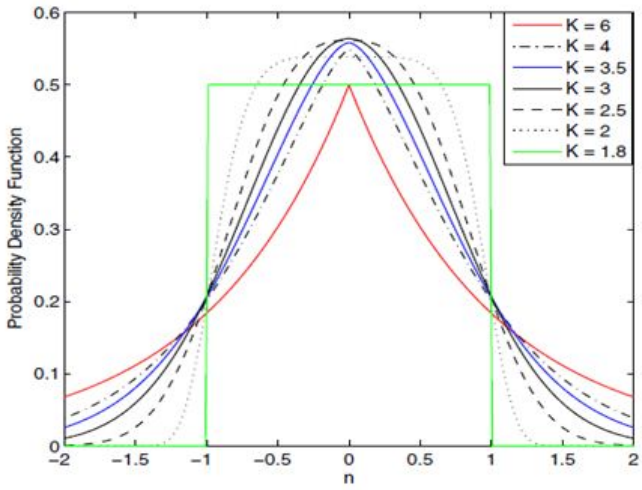

Figure 2.1: Probability density function for different kurtosis values

say as value of shape parameter goes on increasing the distribution becomes more flat-topped tending towards **platykurtic** distribution where we can see they converge towards zero at a faster rate as compared to normal distribution. Noise generated from hydrodynamic process, such as propeller cavitations comes under this category. For low values of shape parameter from the figure we can see the distribution becomes impulsive being taller and tight giving a high kurtosis value and falling under **leptokurtic** category.

- For $\beta = 1$, Eq.2.5 becomes

  $\mathrm{f_{N-GG}\,(n)} = \frac{1}{2\alpha} \exp\left\{-\left(\frac{|\mathrm{n}-\mu_\mathrm{n}|}{\alpha}\right)\right\}$ which is a laplacian distribution.

- For $\beta = 2$, Eq.2.5 becomes

  $f_{N-GG}\,(n) = \frac{1}{\sqrt{\pi\alpha^2}} \exp \exp\left\{-\frac{(n-\mu_n)^2}{\alpha^2}\right\} = N\left(\mu, \frac{\alpha^2}{2}\right)$ i.e. normal distribution with mentioned mean and variance.

- Likewise as β goes on increasing and approaches ∞ the GG PDF coincides with PDF of uniform distribution $u(\mu - \sigma, \mu + \sigma)$.

Typically kurtosis value lies in the range 2 to 4 for oceanic noise. As in UWA communication the main source of noise is generally due to surface waves and shipping so the critical values of kurtosis are 2.5 and 3.5 and the GG distribution can fit to this source by shape parameter value of 2.77 and 1.628 respectively.

The cumulative distribution function is given as,

$$\mathrm{F_{N-GG}\,(n)} = \frac{1}{2} + \mathrm{sgn}\,(\mathrm{n} - \mu_\mathrm{n})\, \gamma_\mathrm{l}\left[\frac{1}{\beta}, \left(\frac{\mathrm{n}-\mu_\mathrm{n}}{\alpha}\right)^\beta\right] \Big/ 2\,\left(\frac{1}{\beta}\right)$$

Where, $\gamma_l()$ is the lower incomplete gamma function which is a special function with incomplete integral limits (0 to some variable upper limit) and is defined as,

$$\gamma_1(s,x) = \int_0^x t^{s-1}e^{-t}dt$$

The CDF plot is given by,

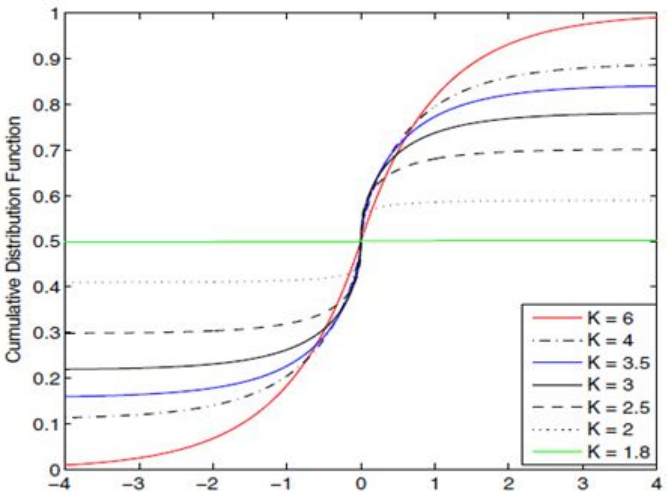

Figure 2.2: Cummulative Distribution Function for different kurtosis values

2.4 GG Distributed Noise Sample Generation

GG random variables are the generalized one and strongly dependent on the shape parameter. There is no inbuilt function for generation GG random variable generation as the CDF expression Eq. 2.8 is having a complex form. So, for generation of GG distributed random variable we need use "Inverse Transform Sampling" method [18].

2.4.1 Inverse Transform Sampling

Inverse transform sampling (also known as golden rule, Smirnov transform or inverse probability integral transform) is a basic method for generating random samples for any probability distribution given its cumulative distribution function. Let us consider a CDF $F(X)$, that may be continuous or non-continuous and we know CDF is always a non-negative and non-decreasing function such that$F : R \in [0,1]$ .In inverse transform sampling method we generate an uniform random variable 'u' with mean zero and unit variance which denotes the probability of occurrence of the random number and from this we will find the largest number x following the distribution $P(X)$ such that p($-\infty \leq$X<)$\leq$u. Indirectly here we are randomly choosing a portion of area under the curve and generation a random number such that exactly this portion of area lies to the left of this. This is achieved by calculating the quantile function which is nothing but inversion of the CDF i.e.$F_X^{-1}(u)$.

Steps for random number generation:

- Generate a random number u from the standard uniform distribution in the interval [0, 1].
- Compute the value x such that $F(X) = u$.
- Take x to be the random number drawn from the distribution described by F i.e. calculate $F_X^{-1}(u)$.

2.4.2 Quantile Function of GG distribution

Considering Eq. 2.8 and following the steps of inverse transform sampling we can say,

- Generate a random number u uniformly distributed with mean zero and unit variance.
- $F_{(N-GG)}(n) = 1/2 + sgn(n-\mu_n)(\gamma_l[1/\beta, ((n-\mu_n)/\alpha)^\beta])/(2\Gamma(1/\beta)) = u$
  $\Rightarrow \mathrm{sgn}\,(\mathrm{n}-\mu_\mathrm{n})\,\gamma_\mathrm{l}\left[\frac{1}{\beta}, \left(\frac{\mathrm{n}-\mu_\mathrm{n}}{\alpha}\right)^\beta\right]\Big/2\,\left(\frac{1}{\beta}\right) = \mathrm{u} - \frac{1}{2}$
  $\Rightarrow sgn(n-\mu_n)\gamma_l[1/\beta, ((n-\mu_n)/\alpha)^\beta] = 2\Gamma(1/\beta) * (u-1/2)$

  According to property of signum function from Eq. (2.10) we can say that,

  1. If $2\Gamma\,(1/\beta) * (u-1/2)\; = 0$, then $n = \mu_n$ (indicating u=0.5)
  2. Else if $2\Gamma\,(1/\beta) * (u-1/2)\; < \mu_n$, then $n < \mu_n$ (indicating u<0.5)
  3. Else $n > \mu_n$ (indicating u>0.5)
- For $n \neq \mu_n$, we will be having some value on the left hand side of Eq. (2.10) and let us denote it by n'. So, $\gamma_l[1/\beta, ((n-\mu_n)/\alpha)^\beta] = n'$ and from this using inverse of incomplete gamma function we can generate random number n distributed according to Eq. (2.5).

The simulation results of generating GG distributed random numbers for different shape parameter values are presented below.
From fig 2.3(a)-(d) we can observe that histogram obtained from the inverse transform sampling method of generating GG distributed random variable coincides point wise with the theoretical PDF curve generated from Eq.(2.5) showing the accuracy of the algorithm. In chapter 4 we are going to use inverse transform sampling method for GG distributed noise generation and will be designing a suitable detector.

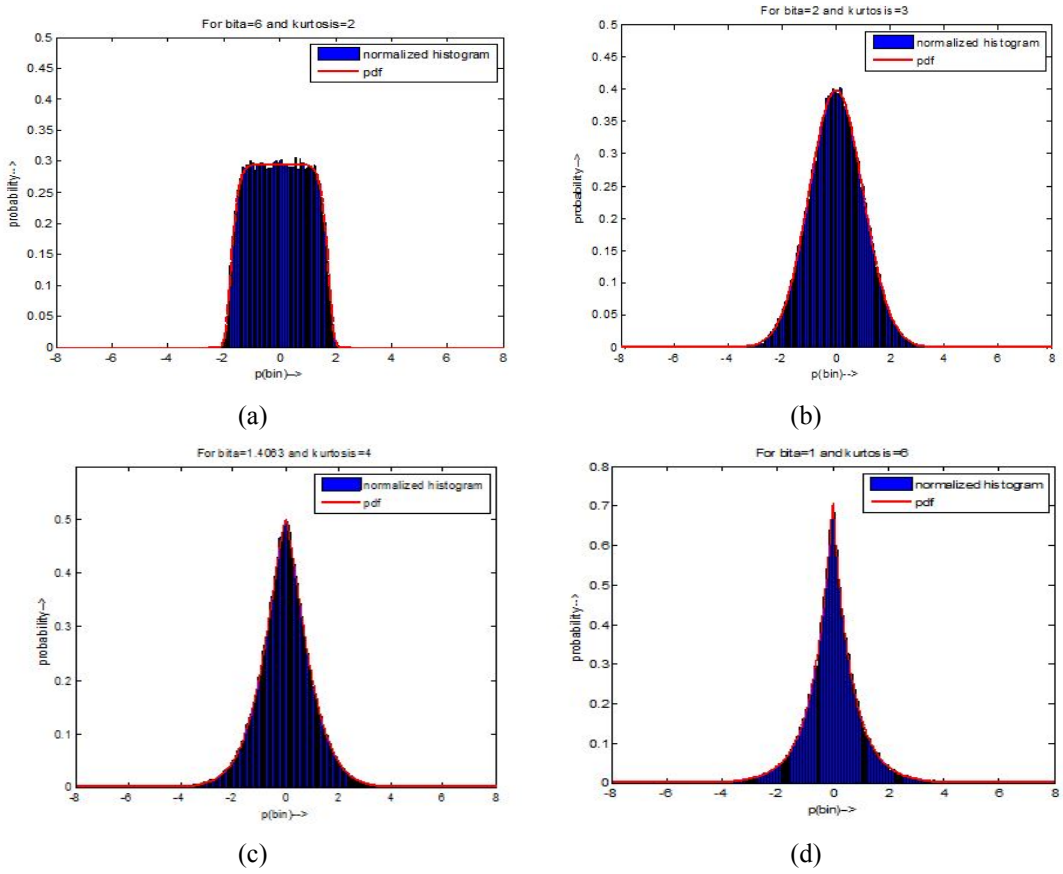

Figure 2.3: Normalized histogram and theoritical PDF comparision (a)$\beta = 6$ and kurtosis=2 (b)$\beta = 2$ and kurtosis=3 (c)$\beta = 1.4063$ and kurtosis=4 (d)$\beta = 1$ and kurtosis=6

Chapter 3

UWA Fading Model

3.1 Preview

In wireless communication, while traveling through the medium the signal experiences effect of channel.In UWA communication due to surface waves, sea bed, rainfall signal undergoes reflection, refraction, scattering etc. leading to multipath propagation [19]. Multipath propagation causes series of replicas of the same transmitted signal at the receiver leading to interference which makes signal exploitation very difficult.As signal travels through multiple paths experiencing different phase delay this rapid phase change causes constructive and destructive interference at the receiver and this leads to rapid variation in signal strength.This phenomena is referred as fading.
The two main causes of multipath in UWA communication are

- **Surface reflection:** This is caused generally due to the horizontal channel faced by the transmitted signal. While transmission the signal faces sea surface which may be rough or smooth, the sea bottom, the irregularity while traveling from sea surface to sensors embedded at the sea surface and any objects that are present in the path.
- **Refraction:** This phenomena is due to spatial variation of sound speed with the depth of the sea. On the sea surface temperature and pressure remains almost constant so as the speed but as depth goes on increasing both of the parameters start varying and show their effect on speed.As the depth goes on increasing temperature starts decreasing and pressure increases.Sound speed being directly proportional to both temperature and pressure,it decreases for this region called as main thermocline.In this range pressure change is not enough to offset this decrease in speed sound. Salinity is also another factor affecting the speed of sound and are directly proportional. According to Snell's law the sound wave bends more in the region of low speed of propagation leading to refraction [8].

3.2 Scales of Fading

In mobile environment as both transmitter and receiver are moving so we can categorize fading into two types depending on the received signal power over distance[20].

3.2.1 Large Scale Fading

It is also called as "shadowing" which is concerned about large distance effects and its effect appears clearly when any of the transmitter and receiver is mobile in nature. Path loss and shadowing generally considered in large scale propagation effect as they occur over relatively larger distance. Received power variation due to shadowing occurs over distances that are proportional to the obstructing object and path loss occurs over long distance (100-1000m).

3.2.2 Small Scale Fading

These variations occur over small distance in the order of the signal wavelength. Here received signal frequency changes due to Doppler Effect. Doppler spread (D) can be calculated as,

$$D = \frac{vf}{c}$$

Where v is the relative speed of the receiver with respect to transmitter, f is the carrier frequency, c is the wave propagation speed which is 1500 m/s for acoustic waves. So Doppler spread is large in UWA communication as compared to radio communication which makes carrier recovery a challenging task. Large Doppler spread leads to small coherence time which implies UWA channel is highly time varying in nature.So as the speed of the terminal increases the received frequency changes rapidly. This is described by slow and fast fading. When a symbol is transmitted and follows multipath then each path undergoes random delay. Since acoustic channel is time-varying in nature so the delay spread becomes a random variable as it is the difference between delay faced by a multipath component and the LOS path delay or the average delay. Generally we define delay spread(μ_{Tm}) by mean and R.M.S. delay spread(σ_{Tm}) because there are some multipath components which are having less power than a given noise floor so they shouldn't contribute significantly in decision making process. These delay spread are obtained by considering the power associated. For classification of small scale fading we consider R.M.S. delay spread as this is good measure of variation about the average delay spread. Another important factor is coherence bandwidth B_c. If we compute autocorrelation of channel impulse response in frequency domain then the range of frequency after which autocorrelation function becomes nearly equal to zero is called as coherence bandwidth and is inversely proporsonal to R.M.S. delay spread.

- **Flat fading:** When R.M.S. delay spread (σ_{Tm}) « symbol duration (T_s) or coherence bandwidth (B_c) » signal bandwidth (B) then the symbol faces almost constant channel i.e. within this bandwidth channel is highly correlated. This is called is flat fading. One advantage of flat fading is channel estimation becomes easy. But the disadvantage is if the symbol faces deep fade then there is no possibility of recovery as the paths will be non-resolvable and we can't apply diversity techniques. This leads to a narrow

band fading model.

- **Frequency selective fading:** When R.M.S. delay spread (σ_{Tm}) » symbol duration (T_s) or coherence bandwidth (B_c) « signal bandwidth (B) then the symbol faces a random channel i.e. within this bandwidth channel is highly uncorrelated. This is called is frequency selective fading. Here each and every frequency component faces a distinct channel. One disadvantage of frequency selective fading is channel estimation is difficult. But the advantage is if any of the multipath components undergoes deep fade then we can recover the same by considering other paths as the paths are clearly resolvable. This leads to a wide band fading model.

As we have studied earlier that UWA channel is highly time varying in nature and coherence bandwidth is very less, this makes the multipath components resolvable and channel is frequency selective in nature. There are many channel estimation techniques which can be used for estimation of the channel impulse response of UWA channel but in this thesis we will use standard fading distribution. The channel estimation techniques can be integrated in future work.

3.3 Fading Distributions

There are different types of distribution which are used to represent the randomness of the channel. Here we will represent some of the distributions.

3.3.1 Rayleigh Fading

- Rayleigh distribution is the radial component of two uncorrelated Gaussian random variables. This is applied to obstructed propagation paths.
- In Rayleigh fading we don't consider dominant LOS path rather all the copies of the transmitted signal are received through non-LOS path. So it assumes that all the received branches have comparable signal strength.
- The PDF is given by,

$$f(h;\sigma) = \frac{h}{\sigma^2} e^{-h^2/2\sigma^2}, h \geq 0$$

  Where, σ is the scale parameter which indicates the spread of the distribution.
- When a complex number is having independent and identically distributed Gaussian with equal variance and zero mean then it can be considered as Rayleigh distributed random variable.
- Rayleigh distribution is the special case of non-centered chi-distribution with two degrees of freedom.

3.3.2 Rician Fading

- Rician fading is a stochastic model which considers the LOS path to be stronger therefore dominant as compared to non-LOS path.
- The PDF of Rician distribution is given by,

$$f(h; v, \sigma) = \frac{h}{\sigma^2} e^{-(h^2+\sigma^2)/2\sigma^2} I_0(hv/\sigma^2), h \geq 0$$

  Where $I_0()$ is the modified Bessel's function of first kind of order zero .
- If Rician (v, σ) ,$R = \sqrt{x^2 + y^2}$ where $x \sim N(vcos\Theta, \sigma^2)$ and $y \sim N(vsin\Theta, \sigma^2)$ are statistically independent normal random variables and θ is any real number.
- If Rician $(v, 1)$, then R has a non-central chi distribution with two degrees of freedom and no central parameter v.
- If Rician $(0, \sigma)$, then $r \sim Rayleigh(\sigma)$.
- For numerical and analytical evaluation of system performance the expression for Rician fading is less convenient, mainly due to occurrence of Bessel's function in the distribution of the received signal amplitude

3.3.3 Nakagami-m Distribution

- Nakagami fading is a more generalized distribution which fits in a better way as compared to other fading models.
- It is generally used to describe the amplitude of received signal after MRC. Summation of multiple independent and identically distributed Rayleigh fading signals leads to Nakagami fading amplitude[16].
- When signal arrives at the receiver through multiple paths their phase are randomly distributed but they form clusters with signals having almost equal delay spread. Nakagami fading describes different clusters of reflected waves with relatively large delay spread which practically occurs in UWA communication.
- The PDF of Nakagami distribution is given by,

$$\mathrm{f(h; m, \omega)} = \frac{2\mathrm{m^m}}{\mathrm{(m)}\,\omega^{\mathrm{m}}} \mathrm{h^{2m-1} e^{-\frac{m}{\omega} h^2}}, h \geq 0$$

  Where 'm' is the shape parameter which controls the severity or depth of amplitude fading and is given by,

$$\mathrm{m} = \frac{[\mathrm{E}\,(h^2)]^2}{\mathrm{var}(h^2)}$$

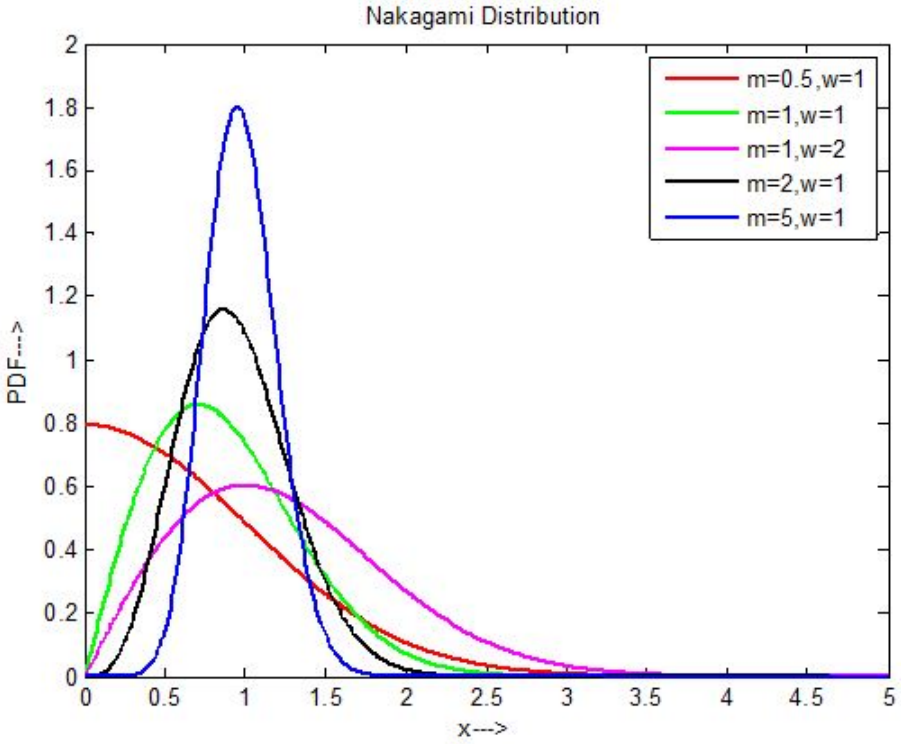

Figure 3.1: Nakagami Probability density function

1. m=1 makes Nakagami distribution equivalent to Rayleigh distribution.
2. m<1 corresponds to more severe fading than Rayleigh fading as the probability that the random variable takes value less than one is more causing deep fade.
3. m>1 corresponds to fading less severe than Rayleigh fading and as m$\rightarrow\ \infty$ it approaches to impulse showing no fading.

The PDF curve of Nakagami distribution for different parametric values is shown below,

From the above figure we can observe if ω will be increased then for the same value of shape parameter the spread will be more. For m=0.5, we can see area covered by the distribution for value less than one is more i.e. the probability that the random variable will take value less than is more causing deep fade. As value of m goes on increasing PDF becomes more impulsive and fading is less severe.

1. If the second moment is held constant then as m approaches infinity Nakagami fading tends to impulse which shows no fading.
2. Mean of Nakagami random variable is given by,

$$\mu = \frac{\left(\mathrm{m}+\frac{1}{2}\right)}{(\mathrm{m})}\left(\frac{\omega}{\mathrm{m}}\right)^{1/2}$$

3. ω is the spread control given by $E[h^2]$ and the variance given by,

$$\sigma^2 = \omega - \frac{\omega}{m}(\frac{\Gamma(m+\frac{1}{2})}{\Gamma(m)})^2$$

4. For integer and half integer values of 'm', the PDF is that of the amplitude of the sum of squared independent Gaussian random variables.

$$R = \sqrt{x_1^2 + x_2^2 ..... + x_n^2}$$

Where x_i, i=1, 2, 3……. n are independent and identically distributed Gaussian random variables with zero mean and equal variance σ_x^2. So Rayleigh fading is a special case of Nakagami-m distribution where $m = \frac{n}{2}$ and $\omega = 2m\sigma_x^2$.

According to the sounding experiment performed at Hudson River estuary[31] where the depth was 3-meter deep and the coverage distance was 505-meter and 200-meter.Then the empirical data is fitted to different statistical model and the closest model is chosen based on distance metrics as given in the table below.If P is the probability of distribution of the measured data and Q is the probability distribution of the fit the the distance metrics are defined as[21],

- Kullback-Leibler divergence=D_{KL}= $D_{KL} = \sum_i P(i)\log_2\frac{P(i)}{Q(i)}$
- Bhattacharyya distance=D_B=$-\log_2 BC$ where Bhattacharyya coefficient,BC=$\sum_i P(i)Q(i)$
- $D_{CRM} = \sqrt{1 - BC}$

Table 3.1: Comparison of fitness of different models to empirical data for 505m

	D_{KL}	D_{BC}	D_{CRM}	**LL**
Gamma	0.0471	0.0041	0.0533	3.14472e+007
Lognormal	0.3689	0.0212	0.1208	3.07348e+007
Beta	0.0439	0.0038	0.0514	3.14567e+007
Rice	0.0413	0.0052	0.0600	3.13174e+007
Rayleigh	0.0413	0.0052	0.0600	3.13174e+007
Nakagami-m	**0.0263**	**0.0037**	**0.0506**	**3.1373e+007**

From table 3.1 we can observe that Nakagami-m distribution is the closest match with m=0.889274.In 200 meter case the value of m for closest matching is 1.0084 but here rician distribution is the closest match which is valid because for short range of communication LOS path is generally significant.But from [14] we concluded that Nakagami-m is the most generalized distribution which can fit to any empirical data with proper shape parameter value.

Table 3.2: Comparison of fitness of different models to empirical data for 200m

	D_{KL}	D_{BC}	D_{CRM}	**LL**
Gamma	0.0529	0.0136	0.0967	1.41509e+007
Lognormal	0.1803	0.0376	0.1604	1.30297e+007
Beta	0.0328	0.0083	0.0755	1.43424e+007
Rice	**0.0069**	**0.0016**	**0.0336**	**1.45580e+007**
Rayleigh	0.0100	0.0026	0.0122	1.45291e+007
Nakagami-m	0.0263	0.0037	0.0506	3.1373e+007

From the above observation it is concluded that Nakagami-m is the most generalized and suitable channel model to represent underwater acoustic channel.In the detector design section we are going to do all the analysis assuming that channel follows Nakagami-m distribution.

Chapter 4

Detector Design(without fading)

An optimal receiver is one that minimizes the probability of error when signal is corrupted by additive noise. While designing a receiver noise PDF plays an important role. When noise is Gaussian we can design an optimal receiver with very low complexity. But when noise is non-Gaussian in nature then there will be tradeoff between complexity and optimality. So while designing this kind of receiver we need to consider sub optimality.

Many suboptimal detectors have been proposed, however when we opt for a receiver with low complexity we need to compromise with performance. The optimal detector requires complex computations imposing limitations for practical implementation. In this research, we will study some of the receivers and their performance in presence of additive non-Gaussian noise and will go through the proposed work starting from a basic threshold detector with low complexity and will do a comparative analysis. The received sample at i^{th} instant can be modeled as,

$$r_i = s_i + n_i, i = 1, 2, ...N \tag{4.1}$$

where, r_i is the received sample, s_i is the transmitted symbol and n_i is the noise sample at i^{th} sampling instant.This samples are collected at the output of the matched filter where each pulse is of duration T_s that is the symbol duration.

4.1 Optimal Detector

Let us consider H_1 is the hypothesis that represents that +B is transmitted i.e. bit 1 and H_0 is the hypothesis that represents that -B is transmitted i.e. bit 0.
$P(r_k/H_1)$: conditional PDF of observed sample, provided '+B' is transmitted
$P(r_k/H_0)$: conditional PDF of observed sample, provided '–B' is transmitted
Employing hypothesis testing and assuming transmitted symbols are equally probable the optimum detector computes the test statistics,

$$\Lambda(r) = \frac{\prod_{k=1}^{N} P(r_k/H_1)}{\prod_{k=1}^{N} P(r_k/H_0)} \lessgtr 1 \tag{4.2}$$

It computes the probability that the received samples fall under which hypothesis. If $P(r_k/H_1) \geq P(r_k/H_0)$ then symbol being transmitted is +B otherwise –B.
Optimum detector has the best performance but needs very complex computation. So we go for suboptimal receivers.

4.2 Suboptimal Detectors

In this section we will study some of the suboptimal detectors [15], their complexity and performance. Here we will do the study by considering noise only. Design while considering effect of channel will be done in section 4.4.

4.2.1 Gaussian/Linear Detector

This is the simplest detector, whose test statistics is,

$$\lambda_{\mathrm{Gauss}} = \sum_{k=1}^{\mathrm{N}} \mathrm{r_k} \tag{4.3}$$

Complexity of operation performed in linear detector is one summation.This detector has one linear decision boundary and don't perform even sub optimally for non-Gaussian noise. This is due to the fact that it doesn't cover the wide decision regions due to heavy tail of impulse noise. So the probability that the decision will lie in the erroneous region is more.

4.2.2 Sign Correlator

If we consider that we have two copies of the same transmitted signal at the receiver then there will be four decision regions for antipodal signal.The test statistics for sign correlator is,

$$\lambda_{\mathrm{SC}} = \sum_{k=1}^{\mathrm{N}} \mathrm{sgn(r_k)} \tag{4.4}$$

where,sgn(n) denotes the signum funtion.Complexity of this detector is one summation and one comparison.

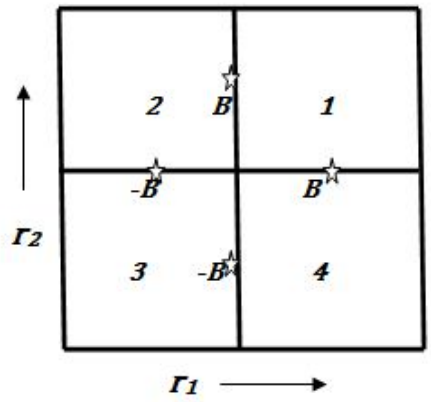

Figure 4.1: Decision region when receiver has two copies of the same transmitted signal

The performance of sign correlator improves if the receiver is supplied with odd number of samples. Because if even number of samples are supplied then from figure 4.1 it can be observed that it performs optimally in 1^{st} and 3^{rd} quadrant. But in 2^{nd} and 4^{th} quadrant sgn(r1) + sgn(r2) =0. So in this region it takes decision as it flips a coin.

4.2.3 Cauchy detector and Myriad Filter

The test statistics is,

$$\lambda_{\text{cauchy}} = \sum_{k=1}^{\text{N}} \log \left[\frac{\text{f}_\text{n}\left(\text{r}_\text{k} + \text{A}\right)}{\text{f}_\text{n}\left(\text{r}_\text{k} - \text{A}\right)} \right] \tag{4.5}$$

Where, A is the transmitted signal amplitude.
$f_n\left(r_k + A\right)$ is the noise PDF when bit '1' is transmitted
$f_n\left(r_k - A\right)$ is the noise PDF when bit '0' is transmitted Complexity in computation is N

division ,N log operations,2N additions.The decision boundary of Cauchy detector fits to the decision boundary of optimal detector. But it provides optimal performance especially for low SNR values and is very complex to be designed.Myriad filter same as that of Cauchy detector but provides optimal performance for high SNR values.

4.2.4 Soft Limiter

In soft limiter we do some processing with the received sample before applying to the Gaussian detector.Here we use a clipping device prior to linear detector which is used to clip the received sample to a certain threshold value. This removes the impulse characteristics of noise from the received sample. The threshold value of the clipping device is calculated in such a way that the outgoing SNR will be maximized.Computational complexity of this detector is one summation and one comparison.Calculation of optimal threshold value to obtain desired performance is very complex.

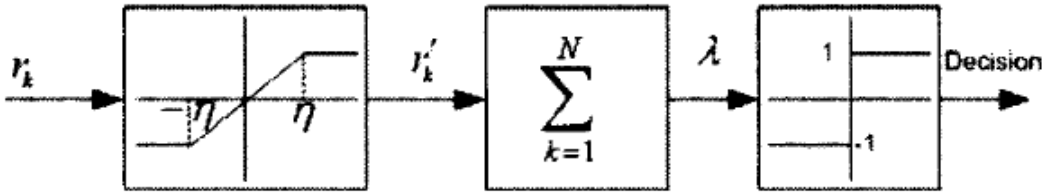

Figure 4.2: diagram of soft limiter

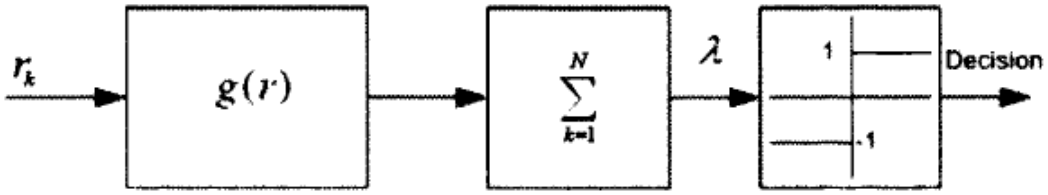

Figure 4.3: diagram of locally optimal bayesian detector

4.2.5 Locally Optimal Bayesian Detector

It applies some nonlinear function to the received sample and that nonlinear function is obtained after applying Taylor series expansion [22] to Eq.(4.5) as,

$$g_{LO} = \frac{-f'(r)}{f(r)} \tag{4.6}$$

It simplifies the test statistics of optimal detector by applying locally optimal theory which is applicable for low SNR values only. So it performs optimally only for low SNR values.Again it needs to take ratio of the derivative of the noise PDF and the noise PDF itself which is very complex.

Now we will do analysis for different receivers. First we will consider a simple threshold/Linear detector and will move towards the proposed detector which performs in a better way than the existing detectors. The analysis and simulation results are presented below.

4.3 Linear Detector

This is the simplest detector that gives decision based on a single threshold value when only one copy of the transmitted signal is available at the receiver. The threshold value is calculated from the noise PDF mean after it is being added to the transmitted signal.
Here we will consider different digital signaling scheme and will derive theoretical probability of error for each individual. Then the performance of the receiver will be studied by using Monte-Carlo simulation.

4.3.1 System Model

Let us consider UWA communication and the received sample at i^{th} instant is,

$$r_i = s_i + n_i, i = 1, 2, ...N$$

where, r_i is the received sample, s_i is the transmitted symbol and n_i is the noise sample at i^{th} sampling instant.These are the samples obtained at the output of the matched filter. Let us consider the noise sample follows GG distribution given in Eq. (2.5) with zero mean and the CDF is represented by Eq. (2.8).Here we assume that only a single noise source is affecting the signal. The CDF for the received sample can be given by,

$$\mathrm{F_r\left(x\right) = p\left(s_i + n_i \leq x\right) = F_{N-GG}\left(x - s_i\right)} \tag{4.7}$$

and the PDF is,

$$\mathrm{f_r\left(x\right) = f_{N-GG}\left(x - s_i\right)} \tag{4.8}$$

so the received signal which is affected by additive GG distributed noise is also a stochastic process which is GG distributed with mean $\mu_r = s_i$, variance is given by $\sigma_r^2 = \frac{N_0}{2}$. Next we will consider different signaling schemes for average probability of error calculation.

4.3.2 Probability of error Calculation

BPSK Signaling

In binary phase shift keying (BPSK) the signal to be transmitted undergoes two phase shifts 0^0 and 180^0 depending on whether the incoming bit is 1 or 0. In BPSK signaling only one bit is transmitted at any time instant. The constellation diagram for BPSK is given in figure 4.4, So for BPSK the received signal can be given by,

$$r = s_i + n = \pm\sqrt{E_b} + n \tag{4.9}$$

so, $r = \sqrt{E_b} + n$ when bit '1' is transmitted
$r = -\sqrt{E_b} + n$ when bit '0' is transmitted
When s1 is transmitted the condition PDF will be equivalent to Eq.(2.5) except change in the mean value.

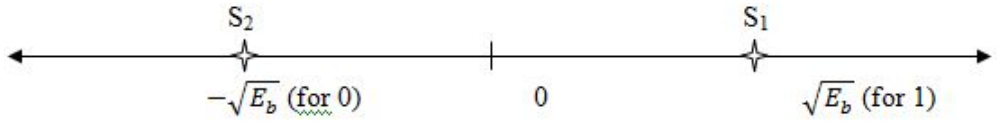

Figure 4.4: BPSK constellation diagram

$$\mathrm{P}\left(\frac{\mathrm{r}}{\mathrm{s}_1}\right) = \frac{\beta}{2\alpha\ (1/\beta)} \exp\left\{-\left(\frac{|\mathrm{r}-\sqrt{\mathrm{E_b}}|}{\alpha}\right)^{\beta}\right\} \tag{4.10}$$

and when s_2 is transmitted

$$\mathrm{P}\left(\frac{\mathrm{r}}{\mathrm{s}_2}\right) = \frac{\beta}{2\alpha\ (1/\beta)} \exp\left\{-\left(\frac{|\mathrm{r}+\sqrt{\mathrm{E_b}}|}{\alpha}\right)^{\beta}\right\} \tag{4.11}$$

The average probability of error can be computed as,

$$\mathrm{P_e} = \frac{1}{2}\mathrm{p}\left(\mathrm{r} < 0/_{\mathrm{s}_1}\mathrm{issent}\right) + \frac{1}{2}\mathrm{p}\left(\mathrm{r} > 0/_{\mathrm{s}_2}\mathrm{issent}\right)$$

$$\Rightarrow \frac{\beta}{4\alpha\ (\frac{1}{\beta})} \int_{-\infty}^{0} [\exp\{-\left(\frac{|\mathrm{r}-\sqrt{\mathrm{E_b}}|}{\alpha}\right)^{\beta} \mathrm{dr} + \exp\{-\left(\frac{|\mathrm{r}+\sqrt{\mathrm{E_b}}|}{\alpha}\right)^{\beta} \mathrm{dr}]$$

$$\Rightarrow P_e = X(Y+Z) \tag{4.12}$$

Now we will evaluate each and every quantity of Eq. (4.12).Considering

$$Y = \int_{-\infty}^{0} exp^{-(\frac{|r-\sqrt{E_b}|}{\alpha})^{\beta}} dr$$

let $r - \sqrt{E_b} = y$. As for s1,$r = \sqrt{E_b} + n$ and goes from $-\infty$ to 0 but as $\sqrt{E_b}$ is always positive so $y = r - \sqrt{E_b}$, is always <0 which implies $|y| = -y$. Then the equation becomes,

$$\int_{-\infty}^{\sqrt{\mathrm{E_b}}} \mathrm{e}^{-\left(\frac{-\mathrm{y}}{\alpha}\right)^{\beta}} \mathrm{dy}$$

Let, $\left(\frac{-\mathrm{y}}{\alpha}\right)^{\beta} = \mathrm{v}$

$$\Rightarrow \frac{-y}{\alpha} = v^{(1/\beta)}$$

$$\Rightarrow \frac{y}{\alpha} = -v^{(1/\beta)}$$

$$\Rightarrow dy = \frac{-\alpha}{\beta} v^{(1/\beta)} dv$$

as $y \to \infty$,$u \to \infty$ and as $y \to -\sqrt{\mathrm{E_b}}$,$u \to \left(\sqrt{\mathrm{E_b}}/\alpha\right)^{\beta}$

the integral now becomes,

$$\frac{-\alpha}{\beta} \int_{\infty}^{\left(\sqrt{\mathrm{E_b}}/\alpha\right)^{\beta}} \mathrm{e}^{-\mathrm{v}} \mathrm{v}^{\frac{1}{\beta}-1} \mathrm{dv}$$

$$= \frac{\alpha}{\beta} \int_{\left(\sqrt{\mathrm{E_b}}/\alpha\right)^{\beta}}^{\infty} \mathrm{e}^{-\mathrm{v}} \mathrm{v}^{\frac{1}{\beta}-1} \mathrm{dv}$$

$$= \frac{\alpha}{\beta} \gamma_u \left[\frac{1}{\beta}, \left(\sqrt{E_b}/\alpha\right)^{\beta}\right] \tag{4.13}$$

where $\gamma_u()$ is the upper incomplete gamma function

From Eq.(2.6), $\alpha = \sqrt{\frac{\sigma_{\mathrm{n}}^2 \left(\frac{1}{\beta}\right)}{\left(\frac{3}{\beta}\right)}}$ and by putting value of σ_n^2 we get,

$$\alpha = \sqrt{\frac{\mathrm{N_0}}{2} \frac{\left(\frac{1}{\beta}\right)}{\left(\frac{3}{\beta}\right)}} \tag{4.14}$$

$$so, Y = \frac{\alpha}{\beta} \gamma_{\mathrm{u}} \left[\frac{1}{\beta}, \left(\frac{\mathrm{E_b}}{\mathrm{N_0}} \frac{2\left(\frac{1}{\beta}\right)}{\left(\frac{3}{\beta}\right)}\right)^{\beta/2}\right] \tag{4.15}$$

Here $\frac{E_b}{N_0}$ is the signal to noise ratio per bit. Now considering s_2, let $r + \sqrt{E_b} = z$. here r goes from 0 to ∞ and $\sqrt{E_b}$ is greater than 0. So, z is always greater than zero which implies $|z| = z$.

Following the same steps as calculation for 'Y' expression for 'Z' is same as that of 'Y' found in Eq. (4.15). Now putting value of 'Y' and 'Z' in Eq. (4.12) we get,

$$P_e = X(Y + Z)$$

$$= \frac{\beta}{4\alpha\Gamma(\frac{1}{\beta})} * 2 * \frac{\alpha}{\beta} \gamma_u [\frac{1}{\beta}, (\frac{E_b}{N0} \frac{2\Gamma(\frac{3}{\beta})}{\Gamma(\frac{1}{\beta})})^{\beta/2}]$$

$$P_e = \frac{1}{2\Gamma(\frac{1}{\beta})} \gamma_u [\frac{1}{\beta}, (\frac{E_b}{N0} \frac{2\Gamma(\frac{3}{\beta})}{\Gamma(\frac{1}{\beta})})^{\beta/2}] \tag{4.16}$$

For $\beta = 2$, the GGD noise becomes standard normal distributed noise. So

$$\alpha = \sqrt{\frac{\sigma_{\mathrm{n}}^2\ (\frac{1}{\beta})}{(\frac{3}{\beta})}} = \sqrt{\frac{\mathrm{N_0}}{2}\frac{(\frac{1}{2})}{(\frac{3}{2})}}$$

$$\Rightarrow \alpha = \sqrt{\frac{\mathrm{N_0}}{2}\frac{\sqrt{\pi}}{\sqrt{\pi/2}}}$$

$$\Rightarrow \alpha = \sqrt{\mathrm{N_0}}$$

Average probability of error can be calculated as,

$$p_e = \frac{2}{2\alpha\Gamma(\frac{1}{2})}\int_{-\infty}^{0} exp - (\frac{|r-\sqrt{E_b}|}{\alpha})^{\beta}dr$$

$$= \frac{1}{\sqrt{\pi N_0}}\int_{-\infty}^{0} exp - (\frac{|r-\sqrt{E_b}|}{\alpha})^{2}dr$$

$$= \frac{1}{\sqrt{\pi N_0}}\int_{-\infty}^{0} exp - (\frac{r-\sqrt{E_b}}{\alpha})^{2}dr$$

Let $\frac{(r-\sqrt{E_b})^2}{N_0} = \frac{x^2}{2}$ i.e. $x = \frac{\sqrt{2(r-\sqrt{E_b})^2}}{N_0}$

$$\Rightarrow 2(r-\sqrt{E_b})dr = xN_0dx$$

$$\Rightarrow dr = \sqrt{\frac{N_0}{2}}dx$$

as $r \to \infty, x \to \infty$ and as $r \to 0\ x \to \sqrt{2E_b/N_0}$ The integral becomes,

$$\mathrm{p_e} = \frac{1}{\sqrt{\pi \mathrm{N_0}}}\int_{\infty}^{\sqrt{2\mathrm{E_b}/\mathrm{N_0}}}\sqrt{\frac{\mathrm{N_0}}{2}}\mathrm{e}^{-\mathrm{x}^2}/2\mathrm{dx}$$

$$\Rightarrow \mathrm{p_e} = \frac{1}{\sqrt{2\pi}}\int_{\infty}^{\sqrt{2\mathrm{E_b}/\mathrm{N_0}}}\mathrm{e}^{-\mathrm{x}^2}/2\mathrm{dx}$$

$$\Rightarrow\ p_e = Q(\sqrt{\frac{2E_b}{N_0}}) \tag{4.17}$$

QPSK Signaling

In quadrature phase shift keying (QPSK) the signal space consist of four constellation points. So these four symbols can be obtained with combination of two bits at a particular time instant. For encoding of these symbols QPSK uses four phase shifts. It uses two carriers in

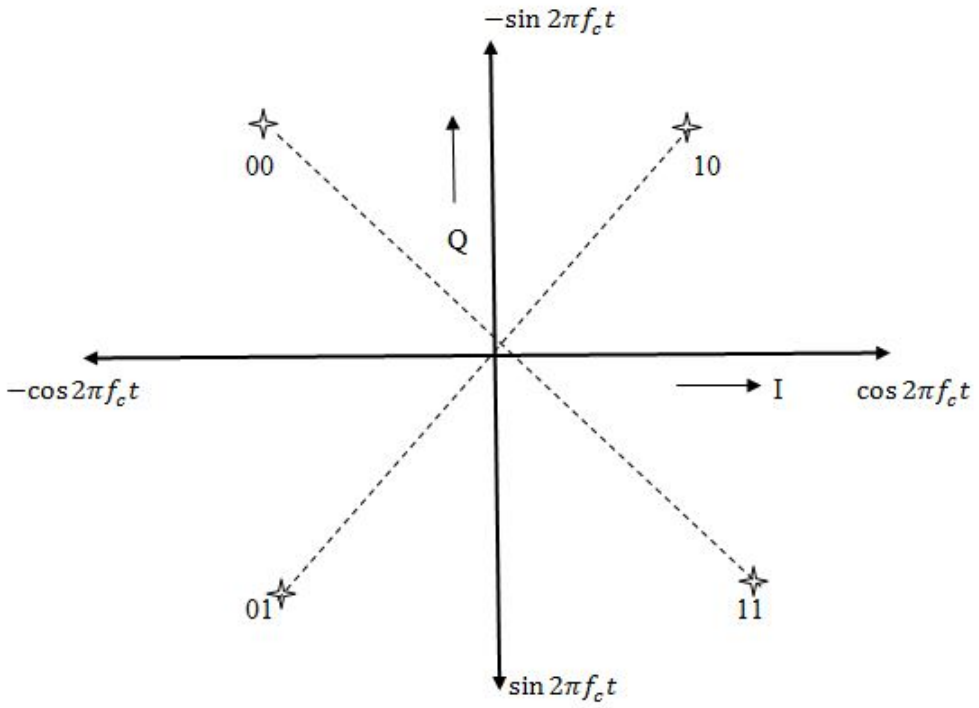

Figure 4.5: QPSK constellation diagram

order to transmit these two bits. One will be in phase carrier and other is quadrature phase carrier. In order to encode the bits in terms of phase we go for gray coding as it undergoes one bit transition between adjacent symbols. Since the bits in a symbol are in quadrature

Table 4.1: Quadrature phase shift keying bit configuration

Symbol	In phase bit	Quadrature phase bit	Phase shift in degrees
0	0	0	135
1	0	1	225
2	1	1	45
3	1	0	315

to each other i.e. independent in nature so they can be thought of two BPSK signals. QPSK doubles the data rate as compared to BPSK with same amount of bandwidth or we can have equal data rate as BPSK with half of the bandwidth.

As we know the in-phase and quadrature-phase bits are independent of each other, so the effects of noise on both of the bits are also independent of each other. If P_e^{BPSK} is the probability that one of the bit is in error then probability of correct reception for the bit is given by (1- P_e^{BPSK}). Since the bits are independent of each other so the probability of correct reception for a QPSK symbol is product of individual bit correct reception probability. So the probability of correct reception of a QPSK symbol is,

$$P_c = (1 - P_e^{BPSK})^2$$

Where P_e^{BPSK} is given by Eq.(4.16). So the probability of error in QPSK is,

$$P_e^{QPSK} = 1 - P_c$$

$$= 1 - \left(1 - \mathrm{P_e^{BPSK}}\right)^2$$

$$= 1 - \left(1 + \left(\mathrm{P_e^{BPSK}}\right)^2 - 2\mathrm{P_e^{BPSK}}\right)$$

$$= 2\mathrm{P_e^{BPSK}} - \left(\mathrm{P_e^{BPSK}}\right)^2$$

$$\mathrm{P_e^{QPSK}} = 2\mathrm{P_e^{BPSK}}\left(1 - \mathrm{P_e^{BPSK}}/2\right) \tag{4.18}$$

By substituting Eq. (4.16) in Eq.(4.18) we get,

$$\mathrm{P_e^{QPSK}} = \frac{1}{\left(\frac{1}{\beta}\right)}\gamma_{\mathrm{u}}\left[\frac{1}{\beta}, \left(\frac{\mathrm{E_b}}{\mathrm{N_0}}\frac{2\left(\frac{1}{\beta}\right)}{\left(\frac{3}{\beta}\right)}\right)^{\frac{\beta}{2}}\right]\left\{1 - \frac{1}{4\left(\frac{1}{\beta}\right)}\gamma_{\mathrm{u}}\left[\frac{1}{\beta}, \left(\frac{\mathrm{E_b}}{\mathrm{N_0}}\frac{2\left(\frac{3}{\beta}\right)}{\left(\frac{1}{\beta}\right)}\right)^{\beta/2}\right]\right\}$$

For $\beta = 2$ Eq.(4.19) will reduce to QPSK probability of error in presence of Gaussian noise. For shape parameter value of 2 we get the scale parameter as $\alpha = \sqrt{N_0}$. So Eq.(2.5) turns to be

$$f_{N-GG}(n) = \frac{1}{\sqrt{\pi N_0}}\exp\left\{-\left(\frac{|n - \mu_n|}{\alpha}\right)^{\beta}\right\}$$

A QPSK symbol is said to be received correctly if and only if both the bits of a symbol are received correctly. Let s_1 i.e. '01', so from fig.(4.5) we can say this symbol is said to be received correctly only if the in-phase component is greater than zero and quadrature-phase component is less than zero i.e. probability of correct reception is given by,

$$\mathrm{P_c} = \mathrm{P(I > 0/s_1 issent)P(Q < 0/s_1 issent)} \tag{4.19}$$

$$\mathrm{P}\left(\mathrm{I} > 0/s_1 issent\right) = \int_0^{\infty} \frac{1}{\sqrt{\pi \mathrm{N_0}}}\exp\left\{-\left(\frac{\left|\mathrm{n} - \sqrt{\mathrm{E_b}}\right|}{\sqrt{\mathrm{N_0}}}\right)^2\right\}\mathrm{dn} \text{ (as } \mu_n \text{ is 0)}$$

$$1 - \int_{-\infty}^{0} \frac{1}{\sqrt{\pi \mathrm{N_0}}}\exp\left\{-\left(\frac{\left|\mathrm{n} - \sqrt{\mathrm{E_b}}\right|}{\sqrt{\mathrm{N_0}}}\right)^2\right\}\mathrm{dn}$$

Let $\frac{\left|n - \sqrt{E_b}\right|}{\sqrt{N_0}} = a \Rightarrow dn = \sqrt{N_0}da$

as $n \to -\infty, a \to -\infty$ and as $r \to 0, x \to -\sqrt{\frac{E_b}{N_0}}$

so,$\mathrm{P_c} = \mathrm{P(I > 0/s_1 issent)} == 1 - \int_{-\infty}^{-\sqrt{(E_b/N_0)}} \frac{1}{\sqrt{\pi N_0}} exp(-a^2)\sqrt{N_0}da == 1 -$

$$\int_{-\infty}^{-\sqrt{(E_b/N_0)}} \frac{1}{\sqrt{\pi}} exp(-a^2)da = 1 - \int_{\sqrt{(E_b/N_0)}}^{\infty} \frac{1}{\sqrt{\pi}} exp(-a^2)da$$

$$\Rightarrow \mathrm{P(I > 0/s_1issent)} = 1 - \frac{1}{2}\mathrm{erfc}\left(\sqrt{\mathrm{E_b/N_0}}\right) \tag{4.20}$$

In QPSK symbol energy is $E_s = 2E_b$ i.e. $E_b = E_s/2$
So,$\Rightarrow \mathrm{P(I > 0/s_1issent)} = 1 - \frac{1}{2}\mathrm{erfc}\left(\sqrt{\mathrm{E_s/2N_0}}\right)$
Probability of correct reception of a QPSK symbol is,

$$P_c = \mathrm{P(I > 0/s_1issent)P(Q < 0/s_1issent)}$$

$$\Rightarrow \mathrm{P_c} = \left[1 - \frac{1}{2}\mathrm{erfc}\left(\sqrt{\frac{\mathrm{E_s}}{2\mathrm{N_0}}}\right)\right]^2$$

$$\Rightarrow \mathrm{P_c} = 1 - \mathrm{erfc}\left(\sqrt{\frac{\mathrm{E_s}}{2\mathrm{N_0}}}\right) + \frac{1}{4}\mathrm{erfc}^2\left(\sqrt{\frac{\mathrm{E_s}}{2\mathrm{N_0}}}\right)$$

So the probability of symbol error is,

$$\mathrm{P_e^{QPSK}} = 1 - \mathrm{P_c}$$

$$\Rightarrow \mathrm{P_e^{QPSK}} = 1 - \left[1 - \mathrm{erfc}\left(\sqrt{\frac{\mathrm{E_s}}{2\mathrm{N_0}}}\right) + \frac{1}{4}\mathrm{erfc}^2\left(\sqrt{\frac{\mathrm{E_s}}{2\mathrm{N_0}}}\right)\right]$$

$$\Rightarrow \mathrm{P_e^{QPSK}} = \mathrm{erfc}\left(\sqrt{\frac{\mathrm{E_s}}{2\mathrm{N_0}}}\right) + \frac{1}{4}\mathrm{erfc}^2\left(\sqrt{\frac{\mathrm{E_s}}{2\mathrm{N_0}}}\right)$$

$$\Rightarrow \mathrm{P_e^{QPSK}} \approx \mathrm{erfc}\left(\sqrt{\frac{\mathrm{E_s}}{2\mathrm{N_0}}}\right) (as \mathrm{erfc}^2\left(\sqrt{\frac{\mathrm{E_s}}{2\mathrm{N_0}}}\right) \to 0) \tag{4.21}$$

This is same as average probability of error for QPSK signaling in presence of standard normal distribution.

4.3.3 Simulation Results and Discussion

Here we will be plotting the SER vs. SNR in dB curve. The SNR is given by,
$SNR = 10log(\frac{E_b}{N_0})$, where e_b is the average energy per bit and $N_0 = 2\sigma_n^2$.
Noise variance is considered to be unity for simulations and bit energy is varied. Shape parameter for GG distributed noise is considered in the range of 2 to 4 as per UWA communication. We have considered a standard correlator or a linear detector which takes decision directly on the basis of mean value of noise PDF after being added to the transmitted symbol. In Monte-Carlo simulation maximum error count is taken as 1000 and performance

of the linear detector for different kurtosis values is observed.

BPSK Signaling

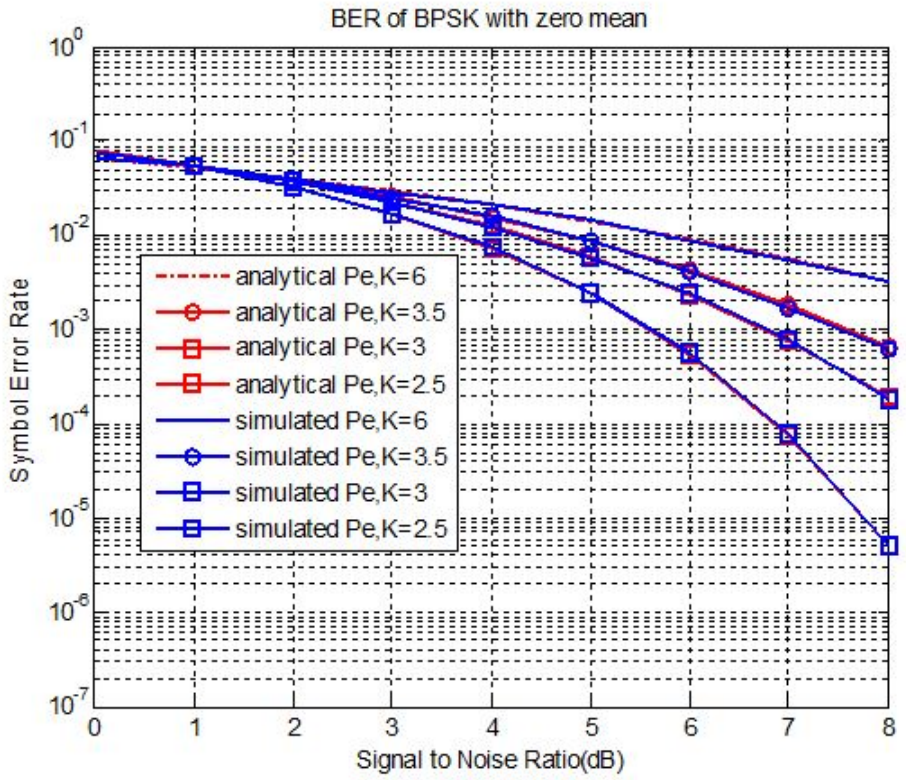

Figure 4.6: BER of BPSK signaling for zero mean of noise

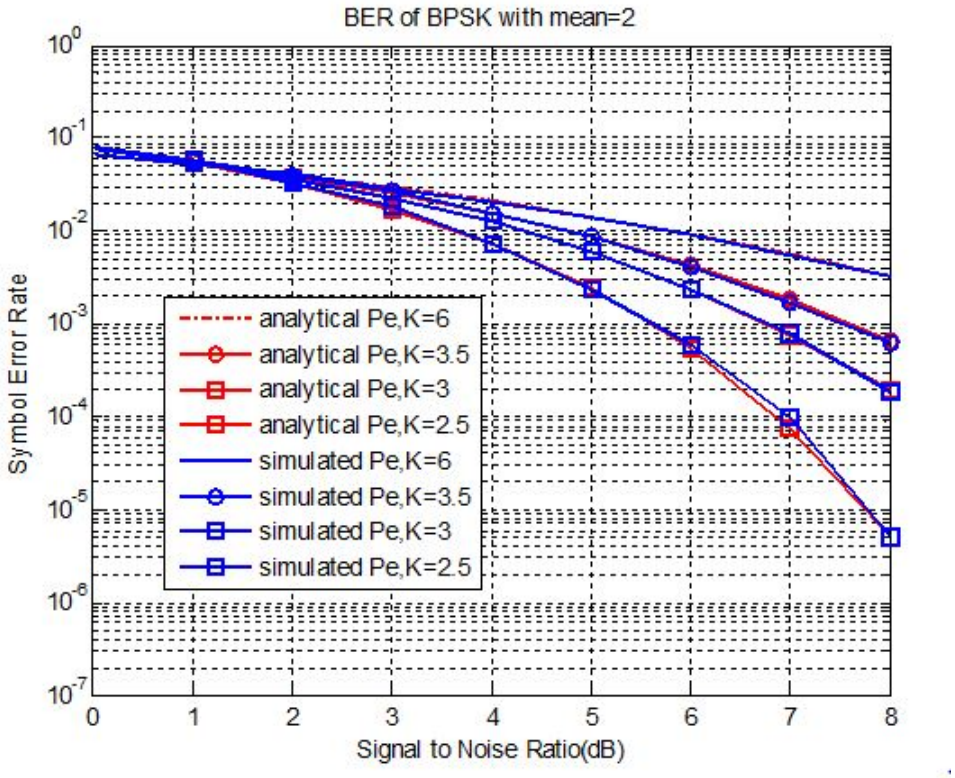

Figure 4.7: BER of BPSK signaling for non-zero mean of noise

From fig (4.6) and (4.7) it is observed that performance of the receiver for zero and non-zero mean of noise is almost similar and it is because of symmetric nature of noise PDF around its mean. Considering fig (4.6) we can observe for kurtosis value of 2.5 it requires around 3.5dB to achieve SER of 10^{-2} and for value of 3, 3.5 and 6 it requires 4.2dB, 4.9dB, 5.6dB respectively. It says clearly that as kurtosis value goes on increasing performance of the receiver degrades from that performance of the receiver in presence of standard normal distribution i.e. kurtosis equals to 3. For K=3.5 receiver requires 7.5dB to achieve SER of 10^{-5} and is improved by 0.7dB for K=3 and by 2dB for K=2.5. The system performs as expected for K=3.

QPSK Signaling

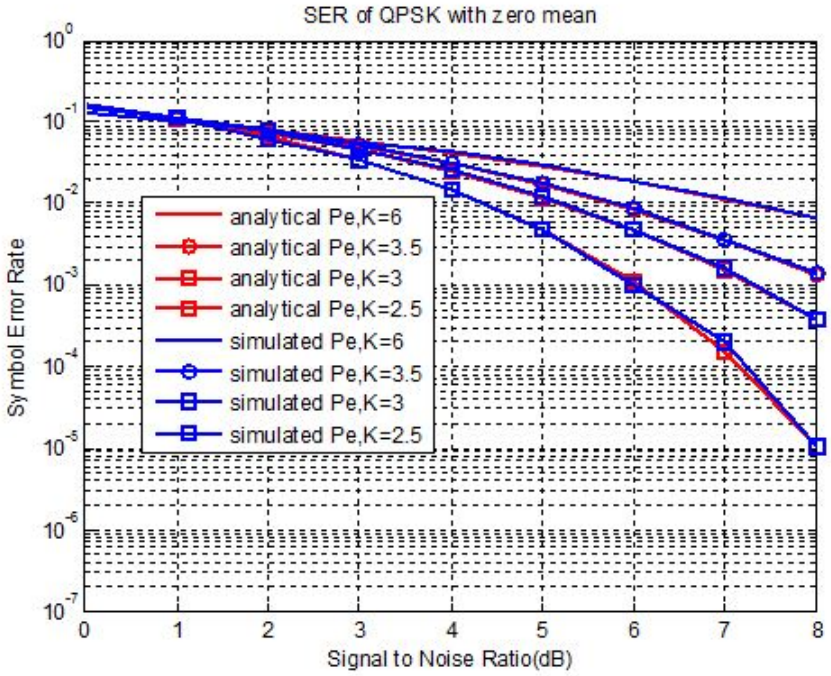

Figure 4.8: BER of QPSK signaling for zero mean of noise

Considering fig (4.8) we can observe for kurtosis value of 2.5 it requires around 4.3dB to achieve SER of 10^{-2} and for value of 3, 3.5 and 6 it requires 5.2dB, 5.8dB, 6.3dB respectively.

For excess kurtosis greater than zero system performance degrades and performance becomes even worse as shape parameter decreases. As kurtosis increases the distribution tends to be impulsive. This standard correlator is unable to achieve the heavy tail characteristics of noise as they decay slowly towards in comparison to standard normal distribution. But for excess kurtosis less than zero system performance becomes better as they have flatter top and decays at a faster rate towards zero. So we need to design a receiver that will give desired performance for any kurtosis value i.e. in any noise environment existing in UWA communication.

In next article we are going to consider presence of multiple noise sources and will propose a receiver design. Presence of multiple interfering sources is quite natural but for simplicity here we will consider two noise sources. Assuming that both the sources are independent of each other the resultant noise will be addition of individual noise sample and resultant noise PDF will be convolution of individual one. This leads to a complex expression very difficult to be analyzed and mathematically intractable. So in order to simplify the analysis we are going to decompose the noise PDF in terms of Gaussian distributions. The resultant PDF will linear weighted combination of Gaussian distribution where the weighting coefficient will give the noise state probability. The technique that will be used for decomposition purpose is “Expectation Maximization Algorithm” that we are going to

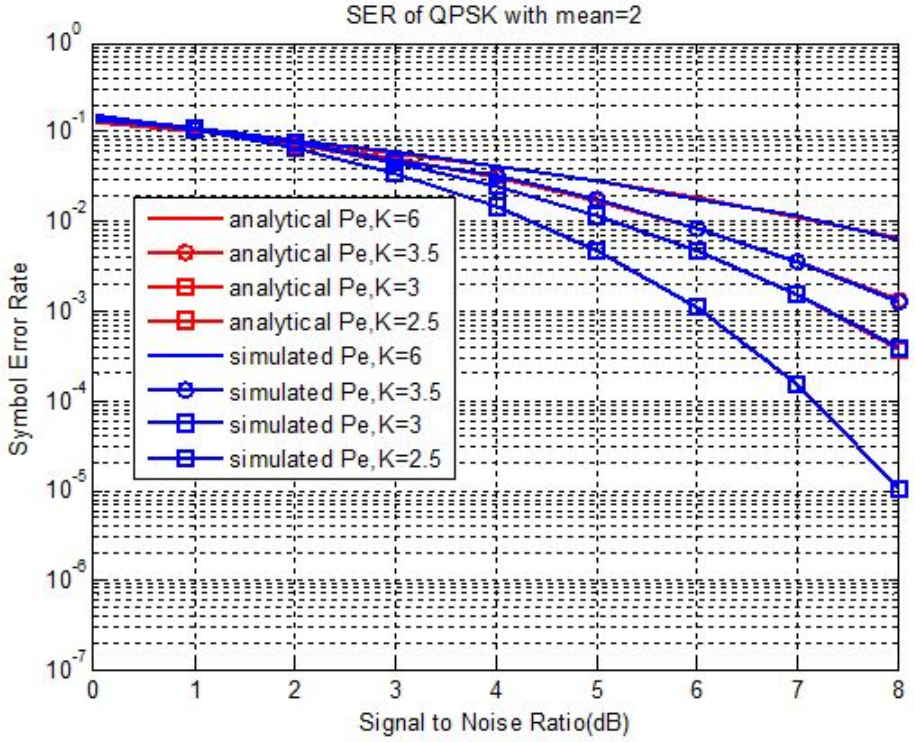

Figure 4.9: BER of QPSK signaling for non-zero mean of noise

discuss in the next section.

4.4 Expectation Maximization Algorithm

Let us consider the received interference to be,

$$X(t) = X_G(t) + X_P(t) \tag{4.22}$$

Where, $X_G(t)$: Gaussian background noise/represents irresolvable background noise and $X_p(t) = \sum_l U_l(t,\theta)$, U_l is the l^{th} waveform from an interfering source and θ represents the random parameter. Let the interfering sources emit interfering waves independently and are Poisson distributed in time. For an interfering source to be Poisson distributed decomposition of noise in terms of Gaussian components[23] can be represented as,

$$\mathrm{P_X\,(x)} = \mathrm{e}^{-\mathrm{A}} \sum_{j=1}^{\infty} \frac{\mathrm{A}^{\mathrm{j}-1}}{(\mathrm{j}-1)!} \frac{1}{\sqrt{2\pi\sigma_{\mathrm{j}}^2}} \mathrm{e}^{-\mathrm{x}^2/2\sigma_{\mathrm{j}}^2} \tag{4.23}$$

$$\sigma_{\mathrm{j}}^2 \approx \frac{\mathrm{j}-1/\mathrm{A}+}{1+} \tag{4.24}$$

4.4.1 Non-structure index/Overlap index

Overlap index 'A' is given by,

$$A = \lambda \bar{T}_m \tag{4.25}$$

λ: Average number of emission on receiver per second
$\bar{T}_m$:mean duration of emission from interfering source
For large value of 'A' the structure in Eq.(4.24) becomes impulsive.

4.4.2 Gaussian Factor (Γ)

Gaussian factor is defined as ratio between the intensity of Gaussian component to the non-Gaussian component of the incoming interference.
Non-structure index and Gaussian factor are two important parameters of structure given in Eq. (4.24), by varying these two we can fit it to great variety of non-Gaussian noise phenomena. Expectation Maximization algorithm [24],[25] mainly focuses on estimation of 'A' and k where $k = A\Gamma$. This is a two step iterative technique for estimating the parameters of the density where the data set is said to be incomplete. A dataset is said to incomplete when it gives idea only about the observation but not about which component of the mixture is occurring at that particular time instant. While observing the samples if we will tag them with a time index then they are turned into complete data set. Let θ denotes the parameter vector to be estimated and $\theta^{(p)}$ is the estimate obtained in p^{th} iteration. x,y represents complete and incomplete data set respectively. The likelihood function associated with x let is denoted by 'g'. so the two steps involved are,

- Expectation step (E-step): Evaluate $\mathrm{Q}\left(\theta/\theta^{(\mathrm{p})}\right) \cong \mathrm{E}\left[\log(\mathrm{g}\left(\mathrm{x}/\theta\right)/z, \theta^{(\mathrm{p})}\right)]$
- Determine $\theta = \theta^{p+1}$ to maximize $Q(\theta/\theta^{p+1})$

So EM algorithm is maximization of 'g' over θ. Since 'g' is unknown we go for maximization of its expected value given observed data and current estimate of parameters. The likelihood function of the incomplete dataset is always monotonically increasing in nature i.e. If 'l' represents the likelihood function then,

$$\mathrm{l}\left(\theta^{(\mathrm{p}+1)}\right) \geq \mathrm{l}\left(\theta^{(\mathrm{p})}\right)$$

This decomposition of GG distributed noise we are going to use in our further analysis.

4.5 Proposed Detector in Presence of Noise Only

4.5.1 System Model

Here we will consider the symbol being transmitted is antipodal in nature i.e. amplitude is $\pm B$ and the noise interfering the transmission is modeled as GG distributed. In this case we will consider that the receiver is supplied with N replicas of the same transmitted symbol which can be realized by using multiple antennas at the receiver or sending the symbol in different time slots. If the noise sample at any time instant is represented by n_k(addition of noise samples from two independent interfering sources) then received signal vector will be, $[r_1, r_2, r_3 \ldots\ldots\ldots\ldots\ldots r_N]$ where $r_k = s_k + n_k$ and $B = \sqrt{E_s} = \sqrt{\frac{E_b}{N}}$ are the output obtained from matched filter. Here we have considered that the noise mean duration is comparable to bit duration in order to maintain independency between the noise samples. If the noise mean duration is greater than the bit duration then there will be dependency between the noise samples in consecutive sampling instants. Let us consider hypothesis H_1 represents signal being transmitted is +B and hypothesis H_0 represents –B.
By EM algorithm the resultant GG noise can be expressed as,

$$\mathrm{p}\left(\mathrm{n_k}\right) = \sum_{m=0}^{\infty} \beta_{\mathrm{m}} \mathrm{g}\left(\mathrm{n_k}; \mu_{\mathrm{m}}, \sigma_{\mathrm{m}}^2\right) \tag{4.26}$$

Where, β_m is the noise state probability and$\mathrm{g}\left(\mathrm{n_k}; \mu_{\mathrm{m}}, \sigma_{\mathrm{m}}^2\right) = \frac{1}{\sqrt{2\pi\sigma_{\mathrm{m}}^2}} \mathrm{e}^{-\frac{(n-\mu_m)^2}{2\sigma_m^2}}$ Here if m=0 it represents the background Gaussian noise stating that no impulse is present. But if $m \geq 1$ then it shows presence of non-Gaussian noise component along with the Gaussian one. Since we have considered the noise samples n_k,k=1,2…N are independent, so the joint PDF of noise will be product of individual noise PDF. So,

$$\mathrm{p}\left(\mathrm{n}\right) = \prod_{k=1}^{\mathrm{N}} \sum_{m=0}^{\infty} \beta_{\mathrm{m}} \mathrm{g}\left(\mathrm{n_k}; \mu_{\mathrm{m}}, \sigma_{\mathrm{m}}^2\right) \tag{4.27}$$

Substituting EQ.(4.28) in Eq.(4.2) we get,

$$\left(\mathrm{r}\right) = \frac{\prod_{k=1}^{N} \sum_{m=0}^{\infty} \beta_{\mathrm{m}} \mathrm{e}^{-\frac{-(r_k-(B+\mu_m))^2}{2\sigma_m^2}}}{\prod_{k=1}^{N} \sum_{m=0}^{\infty} \beta_{\mathrm{m}} \mathrm{e}^{-\frac{-(r_k+(B+\mu_m))^2}{2\sigma_m^2}}} \gtrless 1$$

$$\Rightarrow \ln(\ \left(\mathrm{r}\right)) = \sum_{k=1}^{N} \ln \frac{\sum_{m=0}^{\infty} \beta_{\mathrm{m}} \mathrm{e}^{-\frac{-(r_k-(B+\mu_m))^2}{2\sigma_m^2}}}{\sum_{m=0}^{\infty} \beta_{\mathrm{m}} \mathrm{e}^{-\frac{-(r_k+(B+\mu_m))^2}{2\sigma_m^2}}} \gtrless 0 \tag{4.28}$$

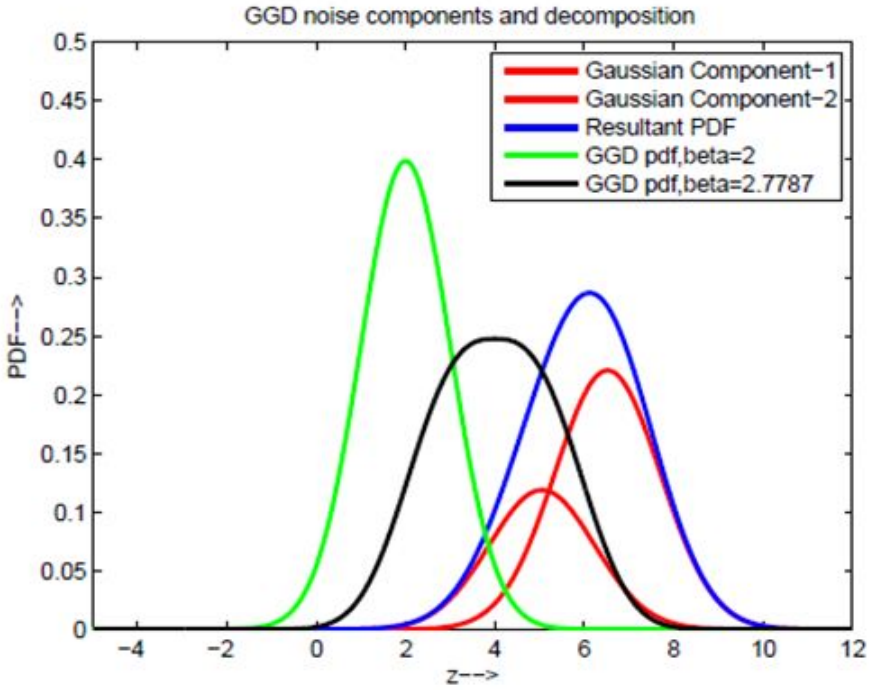

Figure 4.10: Approximation of GG noise for $\beta = 2 and 2.7787$ by two Gaussian components

from Eq.(4.29) we can clearly observe that optimal detector need highly complex computation and impractical to be implemented. So we will go for design of a sub-optimal Maximum Likelihood detector in next article.

4.5.2 Approximated ML Detector with Reduced Complexity

From Eq.(4.24) we get the noise state probability as, $\beta_m = e^{-A}\frac{A^m}{m!}$[26] which shows that it tends to zero as 'm' approaches infinity. In wireless communication it is being observed that the Gaussian mixture model provides a sufficiently accurate approximation to any non-Gaussian noise model for m=2 i.e. by considering two Gaussian terms we can fairly represent our GG distributed noise. For m=2 from the noise state probability of expression we can say for m=0, $\beta_0 = e^{-A}$ and for m=1,$\beta_0 = 1 - e^{-A}$. So the noise in Eq.(4.27) can be well approximated by two Gaussian terms and is given by,

$$\mathrm{p}\left(\mathrm{n_k}\right) \approx \beta_0 \mathrm{g}\left(\mathrm{n_k}; \mu_0, \sigma_0^2\right) + \beta_1 \mathrm{g}\left(\mathrm{n_k}; \mu_1, \sigma_1^2\right) \tag{4.29}$$

By expectation maximization algorithm, considering two noise components with shape parameter 2 and 2.7787 the PDF can be decomposed as, The approximated Gaussian components are having the following parametric values: $\alpha_0 = 0.4212, \alpha_1 = 0.5788, \mu_0 = 4.8562, \mu_1 = 6.8283, \sigma_0^2 = 1.9075, \sigma_1^2 = 2.1844$
The PDF of approximated noise is given by,

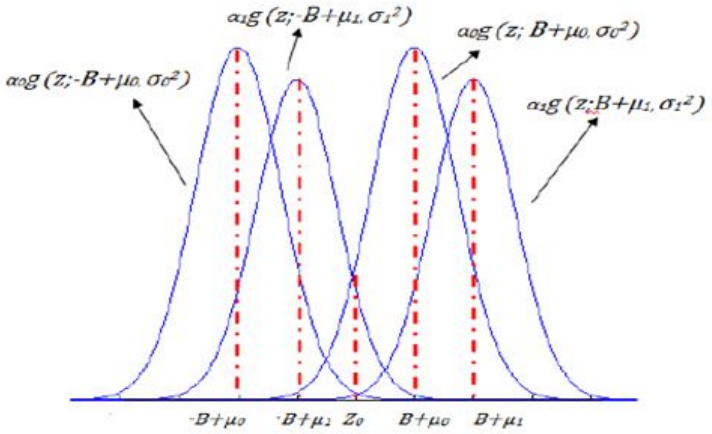

Figure 4.11: Conditional distribution of received signal under Hypothesis H_0 and H_1

We will consider two cases where in one case receiver is having only one copy of the transmitted symbol and another one is when supplied with two copies.

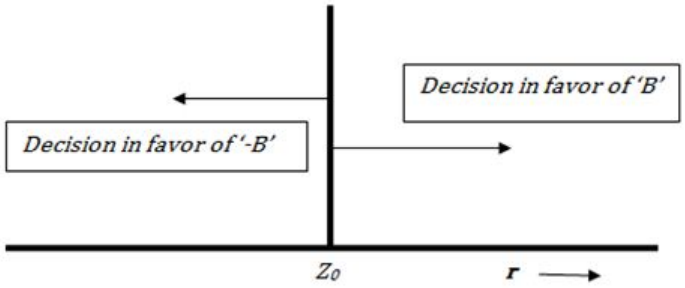

Figure 4.12: Decision boundary with one receiving antenna

When receiver is having one copy of the transmitted signal, then the conditional distribution of received signal under different hypothesis can be expressed as,

$$P(r/H_1) = \beta_0 g(n_k; B+\mu_0, \sigma_0^2) + \beta_1 g(n_k; B+\mu_1, \sigma_1^2) \tag{4.30}$$

$$P(r/H_0) = \beta_0 g(n_k; -B+\mu_0, \sigma_0^2) + \beta_1 g(n_k; -B+\mu_1, \sigma_1^2) \tag{4.31}$$

Figure 4.11 shows the conditional distribution of received signal under assumption of different hypotheses. The decision boundary Z_0 is the threshold point which decides whether decision should be in favor of +B or −B which is shown in figure 4.12 and is computed by equating log likelihood functions, i.e.,

$$\mathrm{l_m}\,(r/H_0) = \ln\left(\frac{\beta_\mathrm{m}}{\sigma_\mathrm{m}}\right) - \frac{(\mathrm{r}-\mu_\mathrm{m}+\mathrm{B})^2}{2\sigma_\mathrm{m}^2} \tag{4.32}$$

$$\mathrm{l_m}\,(r/H_0) = \ln\left(\frac{\beta_\mathrm{m}}{\sigma_\mathrm{m}}\right) - \frac{(\mathrm{r}-\mu_\mathrm{m}-\mathrm{B})^2}{2\sigma_\mathrm{m}^2} \tag{4.33}$$

where, subscript 'm' represents the m^{th} Gaussian. Further, our analysis assume that mean

$\mu_0 < \mu_1$. On putting Eq.4.33 (a)-(b) in Eq.(4.32) and by solving we get the decision boundary Z_0 as,

$$\mathrm{Z}_0 = \frac{\left(\frac{\mu_0}{\sigma_0^2} + \frac{\mu_1}{\sigma_1^2}\right)}{\frac{1}{\sigma_0^2} + \frac{1}{\sigma_1^2}} \tag{4.34}$$

Next, consider the scenario when receiver is with two copies of transmitted signal r = [r1, r2]. Since we have assumed that the copies of received signal are independent of each other, there is a two dimensional decision region. In addition, the distribution of received samples are centered at $(\pm B - \mu_0, \pm B - \mu_0)$,$(\pm B - \mu_1, \pm B - \mu_0)$,$(\pm B - \mu_0, \pm B - \mu_1)$,$(\pm B - \mu_1, \pm B - \mu_1)$ respectively. Thus, decision region can be divided in four quadrants as shown Figure 4.12.

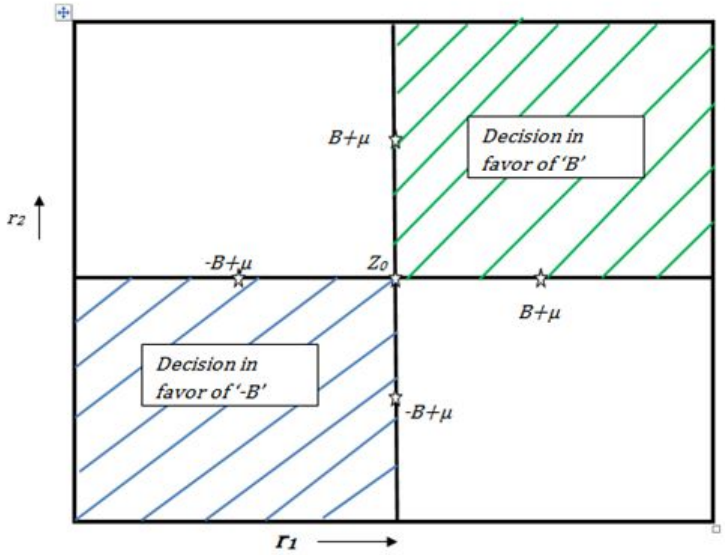

Figure 4.13: Two dimensional decision region for two copies of received signal

It can be observed from the Figure 4.13 that in first and third quadrant both r_1 and r_2 give decision in favor of +B and -B, respectively. So there is no conflict in decision from two copies of received signal. However, for second and fourth quadrant there is conflict in the decision and hence the decision boundary needs to be reanalyzed. For second quadrant, the decision boundary can be computed by equating the corresponding log likelihood functions,

$$l_0\left(r_1/\mathrm{H}_0\right)+\mathrm{l}_1\left(r_1/\mathrm{H}_0\right)=\mathrm{l}_0\left(r_2/\mathrm{H}_1\right)+\mathrm{l}_1\left(r_2/\mathrm{H}_1\right) \tag{4.35}$$

where

$$\mathrm{l}_{\mathrm{m}}\left(r_k/\mathrm{H}_0\right)=\ln\left(\frac{\alpha_{\mathrm{m}}}{\sigma_{\mathrm{m}}}\right)-\frac{\left(\mathrm{r_k}-\mu_{\mathrm{m}}+\mathrm{B}\right)^2}{2\sigma_{\mathrm{m}}^2} \tag{4.36}$$

$$\mathrm{l}_{\mathrm{m}}\left(r_k/\mathrm{H}_1\right)=\ln\left(\frac{\alpha_{\mathrm{m}}}{\sigma_{\mathrm{m}}}\right)-\frac{\left(\mathrm{r_k}-\mu_{\mathrm{m}}-\mathrm{B}\right)^2}{2\sigma_{\mathrm{m}}^2} \tag{4.37}$$

where, subscript 'm' represents the m^{th} Gaussian and 'k' represents the k^{th} receiving antenna. Further, our analysis assume that mean $\mu_0<\mu_1$. After simplification of Eq.(4.65) by using Eq.(4.37) and (4.38) we get,

$r_1{}^2(\frac{1}{\sigma_0^2}+\frac{1}{\sigma_1^2})-2r_1((\frac{-B+\mu_0}{\sigma_0^2})+(\frac{-B+\mu_1}{\sigma_1^2}))+(\frac{-B+\mu_0}{\sigma_0^2})^2+(\frac{-B+\mu_1}{\sigma_1^2})^2=$

$$r_2{}^2(\frac{1}{\sigma_0^2}+\frac{1}{\sigma_1^2})-2r_2((\frac{B+\mu_0}{\sigma_0^2})+(\frac{B+\mu_1}{\sigma_1^2}))+(\frac{B+\mu_0}{\sigma_0^2})^2+(\frac{B+\mu_1}{\sigma_1^2})^2 \tag{4.38}$$

The decision boundary for second quadrant can be plotted from Eq. (4.39) as,

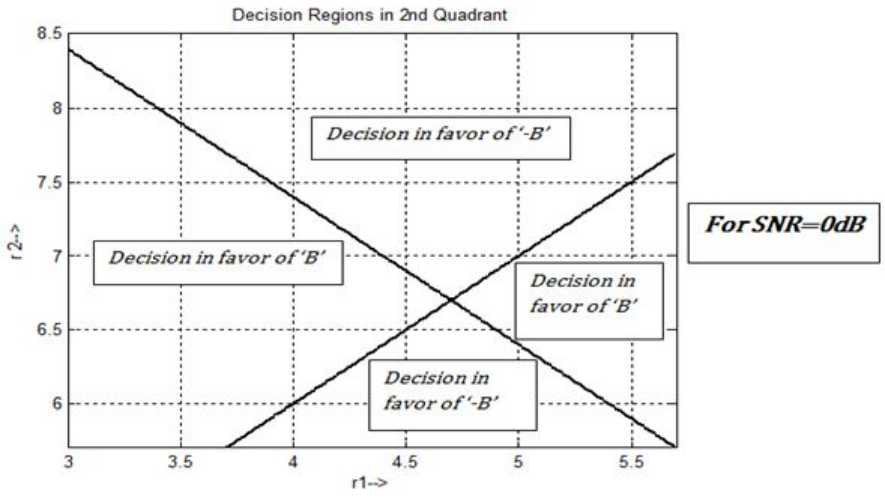

Figure 4.14: Decision boundary for second quadrant in case of two receiving antennas

Here we have plotted the decision boundary for SNR of 0dB. The mean and variance for two GG distributed noise source is taken as (2,1) and (4,2) respectively. From above figure we can observe that the straight line where r_2 increases for decreasing value of r_1 is similar to that of a standard linear detector i.e. for lower side of the straight line it gives decision in favor of r_1 (-B) and for upper side it gives decision in favor of r_2 (+B). But the difference comes from the straight line with opposite slope which gives decision completely different from linear detector. The decisions in all four regions are decided based on the likelihood criterion.

As we will go on increasing the SNR value we will observe that performance of the detector tends towards performance of linear detector. This can be shown in figure 4.15 where as we go on increasing SNR the area covered by the decision region which is in favor of linear detector goes on increasing.

The decision boundary for fourth quadrant is symmetric to that of second quadrant and considering the noise distribution presented in Figure 4.10, the equation for decision region can be found by equating the likelihood

$$l_0\left(r_1/\mathrm{H}_1\right) + \mathrm{l}_1\left(r_1/\mathrm{H}_1\right) = \mathrm{l}_0\left(r_2/\mathrm{H}_0\right) + \mathrm{l}_1\left(r_2/\mathrm{H}_0\right)$$

And the complete decision region (for SNR=0dB) is shown in Figure 4.16.

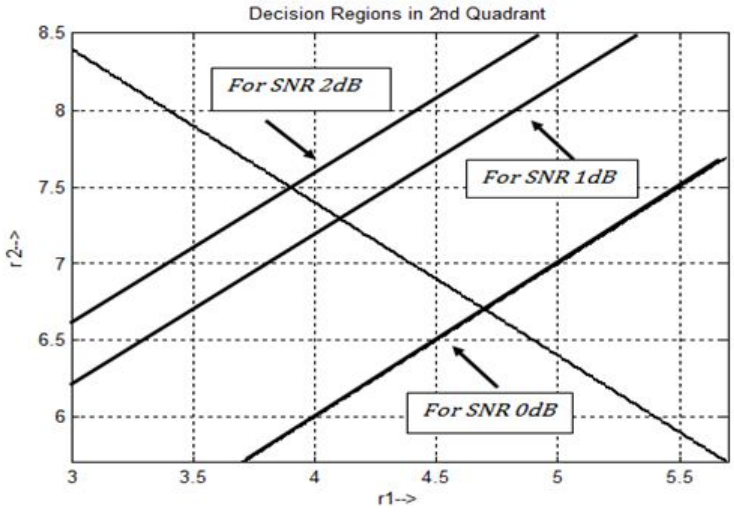

Figure 4.15: Complete Decision boundary with two receiving antennas

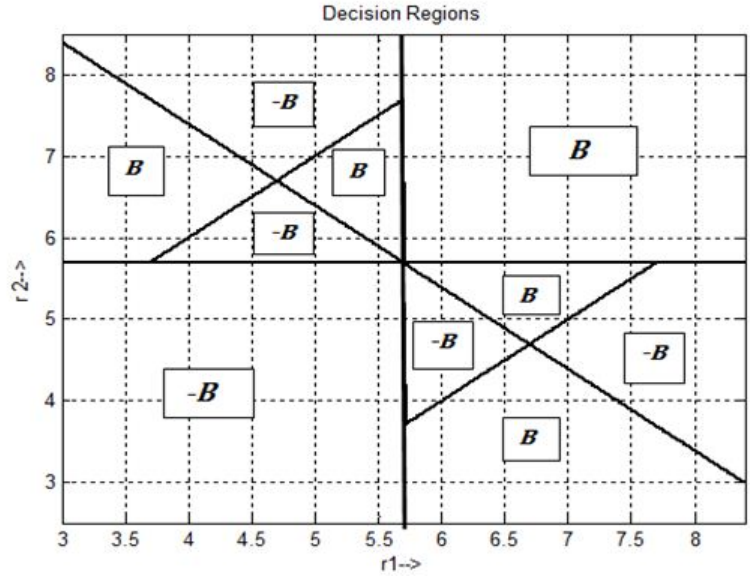

Figure 4.16: Complete Decision boundary with two receiving antennas

4.5.3 Simulation Results and Discussion

Firstly, we discuss simulation result which validates our approach to decompose the UWA channel noise into Gaussian components by EM algorithm. Here we assume BPSK signaling and UWA noise modeled by mixture of two GG distributions with parameters: mean $\mu_0 = 2, \mu_1 = 4$, variance $\sigma_0^2 = 1, \sigma_1^2 = 1$, shape parameter $\beta_0 = 2, \beta_1 = 2.7787$.Figure 4.17 shows the comparison of symbol error rate performance under following detection schemes with the assumption that receiver has only one copy of transmitted signal:

- **Gaussian detector with average threshold:** In this detection mechanism, receiver assumes additive channel noise to be Gaussian distributed with average mean which is used as threshold value for detection,

$$\mu = \frac{\mu_0 + \mu_1}{2} \ and \ \sigma^2 = \frac{\sigma_0^2 + \sigma_1^2}{2}$$

- **Gaussian detector with likelihood based threshold:** In this detection mechanism, receiver assumes additive channel noise to be mixture of two Gaussian distribution with$\mu_0 = 2, \mu_1 = 4, \sigma_0^2 = 1, \sigma_1^2 = 2$.The decision boundary in this case can be computed using equation 4.35.

- **Detector with EM decomposition:** In this detection mechanism, receiver first decomposes the resultant distribution function formed by two GG components into weighted sum of Gaussian densities. The two significant Gaussian destinies have $\beta_0 = 0.4142, \beta_1 = 0.5788, \mu_0 = 4.8562, \mu_1 = 6.8283 \ and \ \sigma_0^2 = 1.9075; \sigma_1^2 = 2.1844$. The decision boundary after this is computed by equation 4.35.

It can be observed from figure 4.17 that Gaussian detector with average threshold is the simplest detector, but it has very poor symbol error rate performance. The performance is improved in Gaussian detector with likelihood based threshold where GG distribution is considered same as Gaussian distribution with same mean and variance parameters. The proposed Detector with EM decomposition shows superior performance compared to other two detectors as the resulting additive noise distribution of UWA communication is suitably approximated by mixture of Gaussian densities. For a SER of 10^{-2} Gaussian detector with likelihood based threshold needs almost 9dB SNR while Detector with EM decomposition needs 2dB less.

Similar, observations can be inferred from Figure 4.18 where receiver is provided with two copies of transmitted signal. Here, threshold for decision boundary is computed by equation 4.35 and decision region is followed from Figure 4.16. Once again it can be verified that by Detector with EM decomposition have superior performance. For a SER of 10^{-2} Gaussian detector with average threshold needs approximately 10 dB SNR, Gaussian detector with likelihood based threshold needs almost 7.6B SNR while Detector with EM decomposition needs 4dB. We can also observe by comparison of figure (4.17) and (4.18) that if the number of sample at the receiver increases then the decision capability of receiver also increases. Here when the number of copies at the receiver increased only by one then the proposed detector needs approximately 3dB less to achieve the same performance.

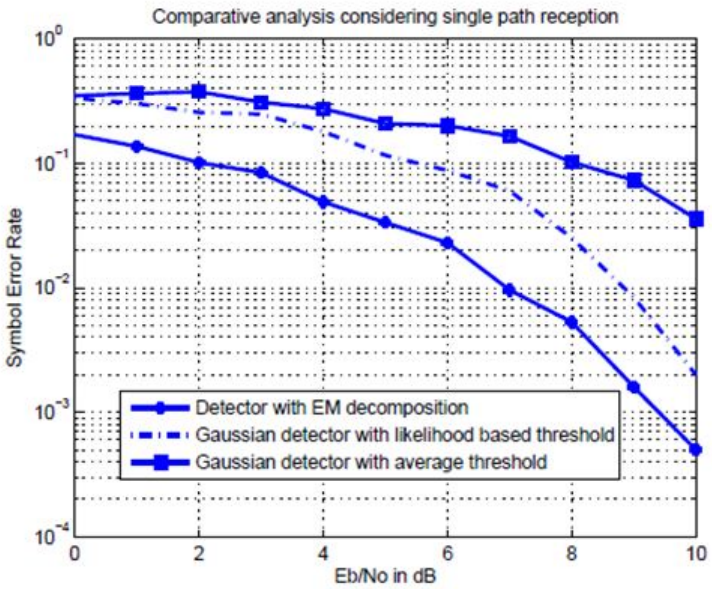

Figure 4.17: Detector performance comparison with single antenna reception

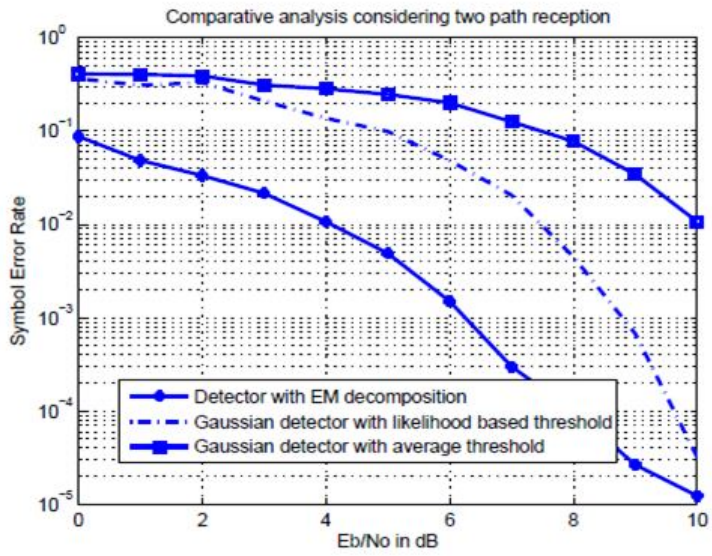

Figure 4.18: Detector performance comparison with two receiving antenna

Finally, we verify the performance improvement obtained by exploiting spatial diversity at the receiver. Figure 4.19 shows symbol error rate performance for UWA noise modeled by mixture of two GG distributions with parameters: shape parameter $\beta_{gg0} = 2, \beta_{gg1} = 2.77$,mean $\mu_{gg0} = 2, \mu_{gg1} = 4$ and variance $\sigma^2_{gg0} = 1, ; \sigma^2_{gg0} = 2$. It can be observed that by having two copies of transmitted signal, there is improvement in symbol error rate performance.

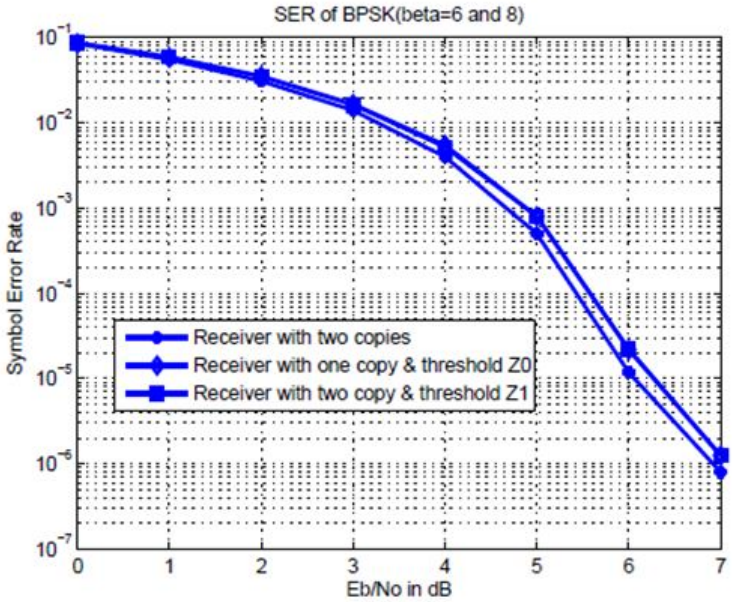

Figure 4.19: Performance improvement via spatial diversity

So from the above analysis we observed that performance of the detector can be improved with increasing number of receiving antenna.When signal is affected by multiple sources of noise which is combination of Gaussian as well as non-Gaussian components it is very difficult to be analyzed mathematically.So it is decomposed in terms of gaussian components which are sufficient enough to follow the heavy tail characteristics of noise.Then the received sample is detected by the maximum likelihood detector which is designed and it can be observed how it outperforms than the linear detectors.

In the next chapter we are going to analyze the signal which is affected by fading also.

Chapter 5

Detector Design(with fading)

Previously we have considered symbol transmission in presence of noise only. Now the effect of fading will also be involved. The channel over here is modeled as Nakagami distributed whose characteristics have already been explained in chapter 2. Here we will consider the symbol being transmitted is antipodal in nature i.e. amplitude is ±B and the noise interfering the transmission is modeled as GG distributed. Similar assumption has made that the receiver is supplied with N replicas of the same transmitted symbol. Let 'h' represents the channel coefficient following Nakagami statistics. The noise sample at any time instant is represented by n_k(addition of noise samples from two independent interfering sources) which is approximated to linear weighted combination of two Gaussian components with appropriate parameters by using EM algorithm as shown in figure 4.10. So,

$$\mathrm{p}\left(\mathrm{n_k}\right) \approx \beta_0 \mathrm{g}\left(\mathrm{n_k}; \mu_0, \sigma_0^2\right) + \beta_1 \mathrm{g}\left(\mathrm{n_k}; \mu_1, \sigma_1^2\right)$$

The GG distributed noise sources are considered with following parameters: mean $\mu_{gg0} = 2, \mu_{gg1} = 4$, variance $\sigma_{gg0}^2 = 0.2, \sigma_{gg1}^2 = 0.8$ and shape parameters $\beta_{gg0} = 2; \beta_{gg0} = 2.77$. The resultant noise distribution is shown in Figure 1. After applying EM algorithm, the resultant noise distribution can be approximated by two Gaussian components with following parameters: $\beta_0 = 0.6696, \beta_1 = 0.3304, \mu_0 = 5.5846, \mu_0 = 6.8398, \sigma_0^2 = 0.7153, \sigma_1^2 = 0.5247$.

The received signal vector at the output of matched filter will be, $[r_1, r_2, r_3 \ldots\ldots\ldots\ldots\ldots r_N]$ where $r_k = \pm hB + n_k$ and $B = \sqrt{E_s} = \sqrt{\frac{E_b}{N}}$. Let us consider hypothesis H_1 represents signal being transmitted is +B and hypothesis H_0 represents –B. Again here also independency between successive samples is maintained.

5.1 Approximated ML Detector with Reduced Complexity

We will consider the scenario when receiver is with two copies of transmitted signal $r = [r_1, r_2]$. The received samples can be expressed as,

$$\mathrm{r_1} = \pm \mathrm{h_1 B} + \mathrm{n_1} \tag{5.1}$$

$$\mathrm{r_2} = \pm \mathrm{h_2 B} + \mathrm{n_2} \tag{5.2}$$

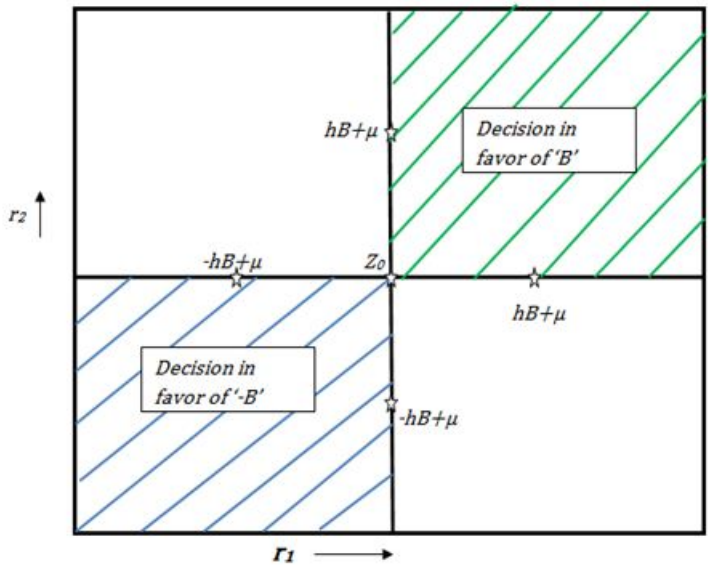

Figure 5.1: Two dimensional decision regions for two copies of received signal affected by channel

Since we have assumed that the copies of received signal are independent of each other, they form a 2-dimensional space. Under hypothesis H_0 and H_1 the received samples are centered at $(-hB+\mu_0, -hB+\mu_0)$,$(-hB+\mu_1, -hB+\mu_1)$,$(hB+\mu_0, hB+\mu_0)$,$(hB+\mu_1, hB+\mu_1 0)$ respectively. Thus, decision region can be divided in four quadrants as shown Figure 5.1. The threshold value Z0 deciding the origin can be calculated by considering any one of the axes. Considering only r1 the PDF of the received sample will look like figure 5.2. The threshold value thus can be calculated by solving the likelihood equation given below,

$$\mathrm{l}_0\left(r_1/\mathrm{H}_0\right) + \mathrm{l}_1\left(r_1/\mathrm{H}_0\right) = \mathrm{l}_0\left(r_1/\mathrm{H}_1\right) + \mathrm{l}_1\left(r_1/\mathrm{H}_1\right) \tag{5.3}$$

where,

$$\mathrm{l}_{\mathrm{m}}\left(r/H_0\right) = \ln\left(\frac{\beta_{\mathrm{m}}}{\sigma_{\mathrm{m}}}\right) - \frac{\left(\mathrm{r} - \mu_{\mathrm{m}} + h_k\mathrm{B}\right)^2}{2\sigma_{\mathrm{m}}^2} \tag{5.4}$$

$$\mathrm{l}_{\mathrm{m}}\left(r/H_1\right) = \ln\left(\frac{\beta_{\mathrm{m}}}{\sigma_{\mathrm{m}}}\right) - \frac{\left(\mathrm{r} - \mu_{\mathrm{m}} - h_k\mathrm{B}\right)^2}{2\sigma_{\mathrm{m}}^2} \tag{5.5}$$

where, subscript 'm' represents the m^{th} Gaussian component and subscript 'k' represents copy of transmitted signal received at k^{th} antenna. Further, our analysis assume that mean $\mu_0 < \mu_1$. On putting Eq.4.40 (a)-(b) in Eq.(4.39) and by solving we get the decision boundary Z_0 as,

$$\mathrm{Z}_0 = \frac{\left(\frac{\mu_0}{\sigma_0^2} + \frac{\mu_1}{\sigma_1^2}\right)}{\frac{1}{\sigma_0^2} + \frac{1}{\sigma_1^2}} \tag{5.6}$$

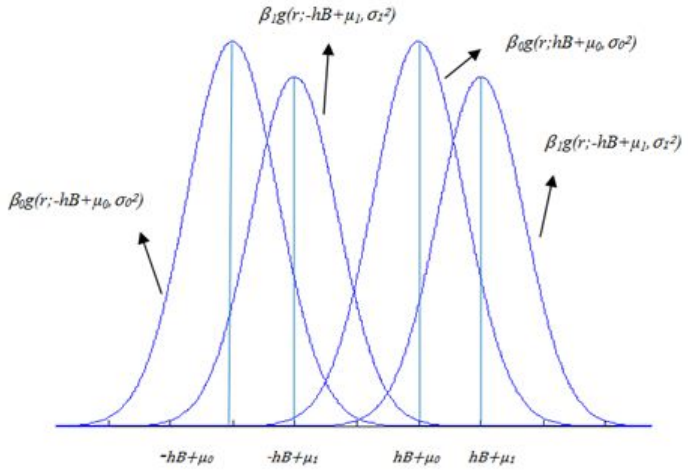

Figure 5.2: Conditional distribution of received signal under Hypothesis H_0 and H_1

This is similar to that of threshold value we got considering noise only. This is because channel coefficient only affects the mean value if the PDF not the point of intersection for different hypothesis. It can be observed from the Figure 5.1 that in first and third quadrant both r_1 and r_2 give decision in favor of +B and -B, respectively. However in second and fourth quadrant there is a conflict in the decision making process so we need to opt for decision boundary analysis in these two quadrants. In second quadrant r_1 gives decision in favor of –B and r_2 in favor of +B. So the decision region in second quadrant can be obtained by solving the likelihood equation,

$$\mathrm{l}_0\left(r_1/\mathrm{H}_0\right)+\mathrm{l}_1\left(r_1/\mathrm{H}_0\right)=\mathrm{l}_0\left(r_2/\mathrm{H}_1\right)+\mathrm{l}_1\left(r_2/\mathrm{H}_1\right) \tag{5.7}$$

Substituting Eq. (5.4) and (5.5) in Eq.5.7 and upon solving we get the result as,

$$r_1{}^2(\frac{1}{\sigma_0^2}+\frac{1}{\sigma_1^2})+2r_1[hB(\frac{1}{\sigma_0^2}+\frac{1}{\sigma_1^2})-\frac{\alpha_0\mu_0}{\sigma_0^2}-\frac{\alpha_1\mu_1}{\sigma_1^2}]-2hB(\frac{\alpha_0\mu_0}{\sigma_0^2}+\frac{\alpha_1\mu_1}{\sigma_1^2})=$$

$$r_1{}^2(\frac{1}{\sigma_0^2}+\frac{1}{\sigma_1^2})+2r_1[hB(\frac{1}{\sigma_0^2}+\frac{1}{\sigma_1^2})+\frac{\alpha_0\mu_0}{\sigma_0^2}+\frac{\alpha_1\mu_1}{\sigma_1^2}]+2hB(\frac{\alpha_0\mu_0}{\sigma_0^2}+\frac{\alpha_1\mu_1}{\sigma_1^2}) \tag{5.8}$$

The decision boundary for second quadrant can be plotted from Eq. (5.8) as, Here we have plotted the decision boundary for SNR of 5dB. The mean and variance for two GG distributed noise source is taken as (2,0.2) and (4,0.8) respectively. From above figure we can observe that the straight line with negative slope is similar to that of a standard linear detector i.e. for lower side of the straight line it gives decision in favor of r_1 (-B) and for upper side it gives decision in favor of r_2 (+B). But the difference comes from the straight line with positive slope which gives decision completely different from linear detector. The decisions in all four regions are decided based on the likelihood criterion.

As we will go on increasing the SNR value we will observe that performance of the detector

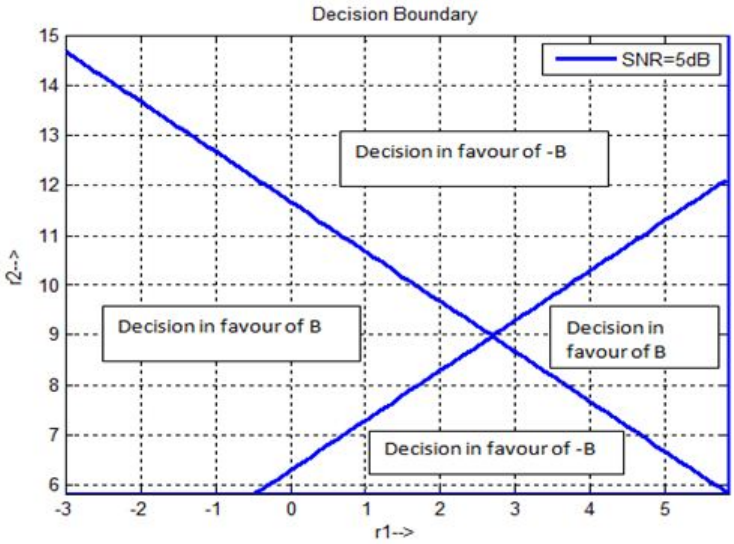

Figure 5.3: Decision boundary for second quadrant in case of two receiving antennas

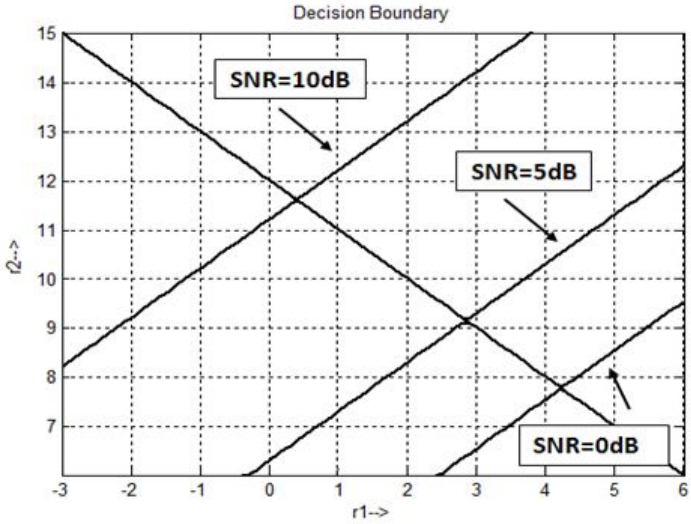

Figure 5.4: Decision region in 2^{nd} quadrant for different SNR values

tends towards performance of linear detector. This can be shown in figure 4.23 where as we go on increasing SNR the area covered by the decision region which is in favor of linear detector goes on increasing.

The decision boundary for fourth quadrant is symmetric to that of second quadrant and considering the noise distribution presented in Figure 4.10, the equation for decision region can be found by equating the likelihood,

$$\mathrm{l}_0\left(r_1/\mathrm{H}_1\right) + \mathrm{l}_1\left(r_1/\mathrm{H}_1\right) = \mathrm{l}_0\left(r_2/\mathrm{H}_0\right) + \mathrm{l}_1\left(r_2/\mathrm{H}_0\right)$$

And the complete decision region (for SNR=5dB) is shown in Figure 5.5.

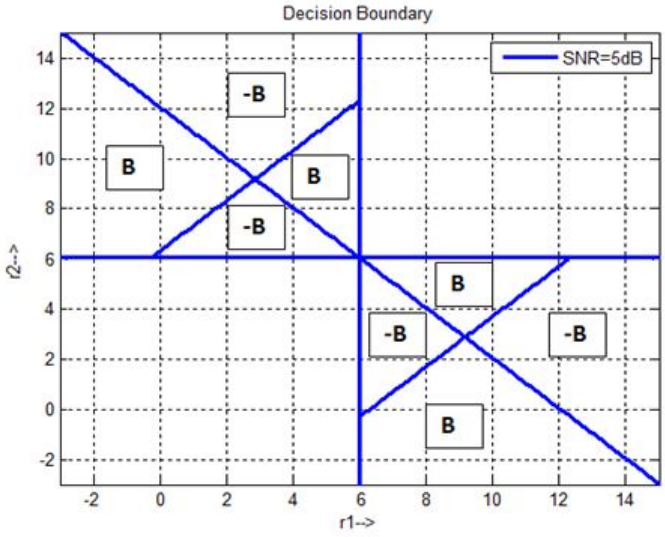

Figure 5.5: Complete decision boundary for two receiving antennas

5.2 Simulation Results

Firstly, we discuss simulation result which validates our approach to decompose the UWA channel noise into Gaussian components by EM algorithm. Here we assume BPSK signaling and UWA noise modeled by mixture of two GG distributions with parameters: mean $\mu_0 = 2, \mu_1 = 4$, variance $\sigma 0^2 = 0.2, \sigma 1^2 = 0.8$,shape parameter $\beta 0 = 2, \beta_1 = 2.7787$. Figure 5.6 shows the comparison of symbol error rate performance under following detection schemes with the assumption that receiver has two copies of transmitted signal:

- **Detector with EM decomposition:** In this detection mechanism, receiver first decomposes the resultant distribution function formed by two GG components into weighted sum of Gaussian densities. The two significant Gaussian destinies have$\beta_0 = 0.6696, \beta_1 = 0.3304, mean\mu_0 = 5.5846, \mu_1 = 6.8398 and \sigma 0^2 = 0.7153, \sigma 1^2 = 0.5247$. The decision boundary after this is computed by equation 5.6.

- **Maximal Ratio Combiner:** Multipath component of a transmitted symbol causes random delay and phase shift to the signal causing in constructive and destructive interference. MRC takes advantage of the multipath reception by multiplying each received branch with a complex coefficient such that the phase shift faced by that branch gets nullified. The complex coefficient is multiplied mainly for co-phasing. This coefficient also decides which branch should contribute more to the decision making process depending on the fading occurred to it [27],[19]. From the above figure we can observe for lower SNR values Detector with EM decomposition outperforms than MRC detector. But as we go on increasing SNR from figure 5.4 we have observed that it approaches towards linear detector. For approaching towards

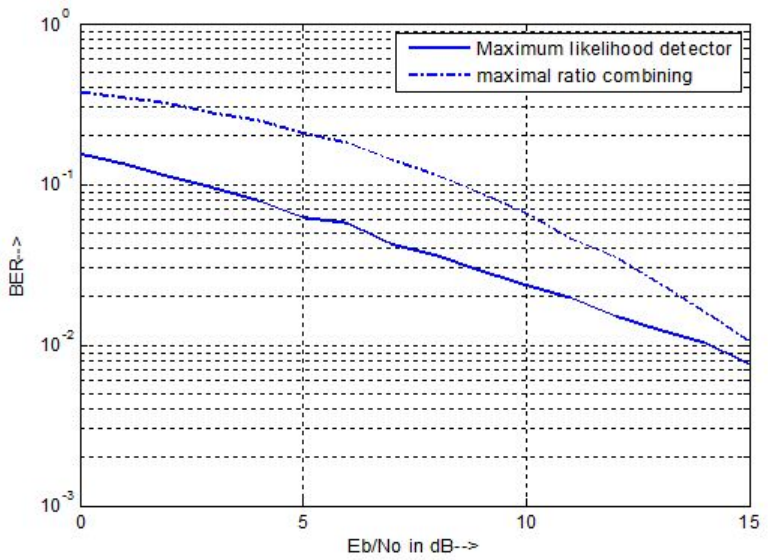

Figure 5.6: Performance comparison between proposed detector and MRC detector

MRC detector the reason is after coherent combination of received branches MRC detector do decision based on a single threshold value as we do in linear detector. But from above figure we can observe to achieve even SER of 10^{-2} we need a very high SNR. This can be reduced to some extent by employing selection combining along with these detectors.

- **Selection combining:** it is a technique which exploits diversity in order to improve performance of the receiver to further extent. When antennas are sufficiently spaced to be independent of each other there is a very rare probability that each of them will undergo deep fade. By selecting one signal among them with highest instantaneous SNR gives better performance than using single antenna at the receiver [27].

Figure 5.7shows the simulation results after employing selection combining with previous detectors. Here we have considered four path reception and among those two branches with maximum instantaneous SNRs are selected. Because of more diversity order ML detector with selection combine gives better performance than ML detector alone. But for higher SNR MRC with SC performs better than ML with SC. So at higher SNR we can achieve better performance by employing MRC with SC detector, but SNR of 8dB is very high to be used. If we will increase the number of receiving antenna let eight antennas are used then the crossing of BER will occur at much low SNR but it is not possible to implement these many antennas at the receiver as the frequency of operation in UWA communication is in the order of KHz. This causes a large spacing between the antennas at the receiver to be independent of each other.

Finally we will compare performance of the proposed detector for various values of shape parameter of Nakagami fading.

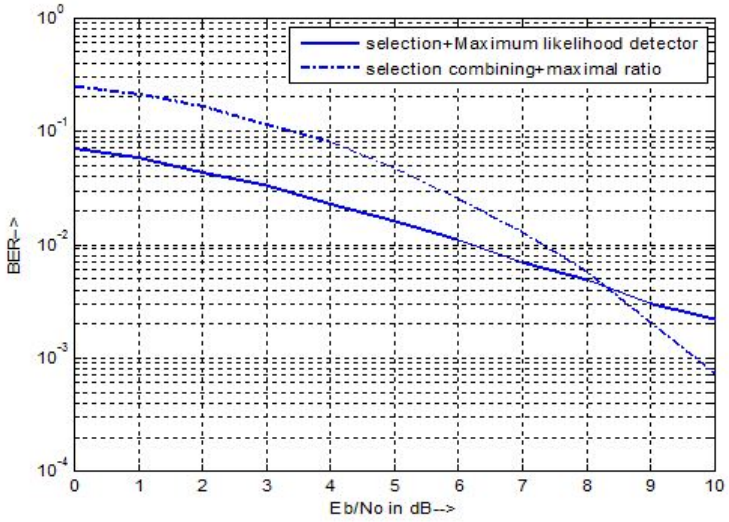

Figure 5.7: Performance comparison between proposed detector and MRC detector along with selection combining

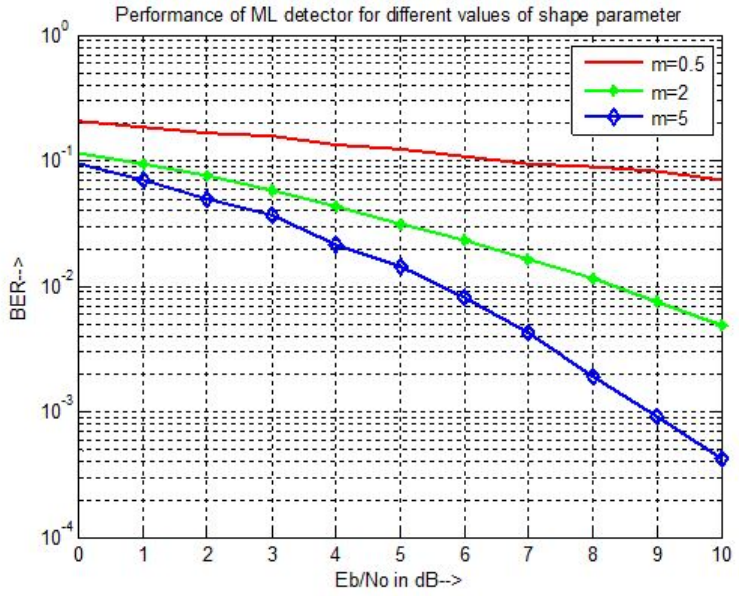

Figure 5.8: Performance comparison of ML detector for different values of shape parameter of fading

Fig.4.27 shows comparison between ML detector performances for different values of shape parameter. As we know for lower values of shape parameter for a given control spread the probability that the channel gain will take values less than '1' is higher and due to this the detector performance is poor in comparison for higher values of shape parameter values where the probability of gain value less than '1' is lower. So here we can observe the detector performance for channel from severe fading i.e. for m=0.5 to less severe fading m=2 and 5. So from the above analysis we observed that performance of the detector can be improved with increasing number of receiving antenna.When signal is affected by multiple sources of noise which is combination of Gaussian as well as non-Gaussian components it is very difficult to be analyzed mathematically.So it is decomposed in terms of gaussian components.Then the received sample is detected by the maximum likelihood detector which is designed and its performance is superior to existing MRC detector which is nothing but behaves like a linear detector after coherent combining.

Chapter 6

Conclusion and Future scope

6.1 Conclusion

In this work we have computed close form expression of decision boundary for detecting binary phase shift keying (BPSK) modulated signals in under water acoustic (UWA) channel. The additive noise is modeled as mixture of GG densities and further approximated by weighted sum of Gaussian densities using expectation Maximization (EM) algorithm. In order to improve the error performance, spatial diversity is exploited by having multiple antennas at receiver. The simulation results validate the approach by indicating improvement in BER performance when compared with traditional detectors. We have observed that this proposed detector is superior to that of threshold detector and the performance can be further improved if the number of copies available at the receiver will increase. Again we have computed close form expression of decision boundary for detecting binary phase shift keying (BPSK) modulated signals in presence of channel that is represented by Nakagami statistics whose shape parameter specifies the depth of fading. In order to improve the error performance, spatial diversity is exploited by having multiple antennas at receiver. Performance of the proposed detector is compared with conventional detectors and its efficiency is observed.

6.2 Future Scope

The detector proposed here is estimating the symbol based on likelihood function. We have exploited only receiver diversity over here. In order to increase the data rate we can integrate MIMO-OFDM and efficient channel equalization techniques in order to improve the detector performance further.

References

[1] M. Stojanovic, "Underwater acoustic communications," in *Electro/95 International. Professional Program Proceedings.* IEEE, 1995, pp. 435–440.

[2] P. Blondel, *The handbook of sidescan sonar*. Springer Science & Business Media, 2010.

[3] M. Stojanovic, "Underwater acoustic communications: Design considerations on the physical layer," in *Wireless on Demand Network Systems and Services, 2008. WONS 2008. Fifth Annual Conference on*. IEEE, 2008, pp. 1–10.

[4] J. Heidemann, W. Ye, J. Wills, A. Syed, and Y. Li, "Research challenges and applications for underwater sensor networking," in *Wireless Communications and Networking Conference, 2006. WCNC 2006. IEEE*, vol. 1. IEEE, 2006, pp. 228–235.

[5] M. Stojanovic, "Recent advances in high-speed underwater acoustic communications," *Oceanic Engineering, IEEE Journal of*, vol. 21, no. 2, pp. 125–136, 1996.

[6] S. Joshy and A. Babu, "Capacity of underwater wireless communication channel with different acoustic propoagation loss models," *International Journal of Computer Networks & Communications (IJCNC)*, vol. 2, 2010.

[7] A. C. Singer, J. K. Nelson, and S. S. Kozat, "Signal processing for underwater acoustic communications," *Communications Magazine, IEEE*, vol. 47, no. 1, pp. 90–96, 2009.

[8] M. Stojanovic and J. Preisig, "Underwater acoustic communication channels: Propagation models and statistical characterization," *Communications Magazine, IEEE*, vol. 47, no. 1, pp. 84–89, 2009.

[9] B. Møhl, M. Wahlberg, P. T. Madsen, A. Heerfordt, and A. Lund, "The monopulsed nature of sperm whale clicks," *The Journal of the Acoustical Society of America*, vol. 114, no. 2, pp. 1143–1154, 2003.

[10] J. C. Goold and P. J. Fish, "Broadband spectra of seismic survey air-gun emissions, with reference to dolphin auditory thresholds," *The Journal of the Acoustical Society of America*, vol. 103, no. 4, pp. 2177–2184, 1998.

[11] D. Middleton, "Non-gaussian noise models in signal processing for telecommunications: new methods an results for class a and class b noise models," *Information Theory, IEEE Transactions on*, vol. 45, no. 4, pp. 1129–1149, 1999.

[12] D. W. Stein, "Detection of random signals in gaussian mixture noise," *Information Theory, IEEE Transactions on*, vol. 41, no. 6, pp. 1788–1801, 1995.

[13] M. Novey, T. Adali, and A. Roy, "A complex generalized gaussian distribution—characterization, generation, and estimation," *Signal Processing, IEEE Transactions on*, vol. 58, no. 3, pp. 1427–1433, 2010.

[14] S. Banerjee and M. Agrawal, "Underwater acoustic noise with generalized gaussian statistics: Effects on error performance," in *OCEANS-Bergen, 2013 MTS/IEEE*. IEEE, 2013, pp. 1–8.

[15] T. S. S. M. Saleh, "Receiver design for signals in non-gaussian noise: Applications to symmetric alpha-stable and middleton's class-a noise models," Ph.D. dissertation, Carleton University Ottawa, 2012.

[16] N. C. Beaulieu and C. Cheng, "Efficient nakagami-m fading channel simulation," *Vehicular Technology, IEEE Transactions on*, vol. 54, no. 2, pp. 413–424, 2005.

[17] B. Tomasi, L. Toni, P. Casari, L. Rossi, and M. Zorzi, "Performance study of variable-rate modulation for underwater communications based on experimental data," in *OCEANS 2010*. IEEE, 2010, pp. 1–8.

[18] K. Sigman. (2010) inverse transform sampling. [Online]. Available: www.columbia.edu/~ks20/4404-Sigman/4404-Notes-ITM.pdf

[19] A. Goldsmith, *Wireless Communications*. Cambridge University press, 2005.

[20] J. G. P. A. Radosevic and M. Stojanovic, "Statistical characterization and capacity of shallow water acoustic channels," *OCEANS 2009 - EUROPE, Bremen*, pp. 1–8, 2009.

[21] B. Borowski, "Characterization of a very shallow water acoustic communication channel," *OCEANS 2009,Biloxi, MS*, pp. 1–10, oct 2009.

[22] S. Rappaport and L. Kurz, "An optimal nonlinear detector for digitaldata transmission through non-gaussian channels," *IEEE Trans. Commun. Technol.*, vol. 14, no. 3, p. 266–274, jun 1996.

[23] S. M. Zabin and H. V. Poor, "Efficient estimation of class a noise parameters via the em algorithm," *IEEE Trans. Inf. Theory*, vol. 37, no. 1, pp. 60–72, jan 1991.

[24] A. P. D. N. M. L. D. B. Rubin, "Maximum likelihood from incomplete data via the em algorithm," *Journal of the Royal Statistical Society. Series B (Methodological)*, vol. 39, no. 1, pp. 1–38, 1977.

[25] K. H. K. A. Saaifan and W. Henkel, "Efficient nonlinear detector of binary signals in rayleigh fading and impulsive interference," *Vehicular Technology Conference (VTC Fall), 2012 IEEE, Quebec City, QC*, pp. 1–5, 2012.

[26] W. H. A. Saaifan, "Decision boundary evaluation of optimum and suboptimum detectors in class-a interference," *IEEE TRANSACTIONS ON COMMUNICATIONS*, vol. 61, no. 1, pp. 1–10, jan 2013.

[27] M. Z. Win and J. H. Winters, "Analysis of hybrid selection/maximal-ratio combining of diversity branches with unequal snr in rayleigh fading," *Vehicular Technology Conference, 1999 IEEE 49th, Houston, TX,*, vol. 1, pp. 215–220, 1999.

[28] N. Kong and L. B. Milstein, "Average snr of a generalized diversity selection combining scheme," *IEEE Communications Letters*, vol. 3, no. 3, pp. 57–59, mar 1999.

[29] K. A. Saaifan and W. Henkel, "A spatial diversity reception of binary signal transmission over rayleigh fading channels with correlated impulse noise," *Telecommunications (ICT), 2012 19th International Conference on, Jounieh*, pp. 1–5, 2012.

[30] D. C. J.G.Proakis, *Digital Communications*, 4th ed. McGraw-Hill, NY, 2000.

[31] S. Haykin, *Communications Systems*, 4th ed. John Wiley & Sons, INC, 2001.

Dissemination

1. Snigdha Bhuyan and Siddharth Deshmukh," Decision Boundary for Under Water Acoustic Communication with Generalized Gaussian Noise Model", International Conference on Signal Processing and Communications (SPCOM)- 2016.(Accepeted)
2. Snigdha Bhuyan and Siddharth Deshmukh ,"A ML Detection for UWA Communication with Nakagami Fading and GG Noise", Third Underwater Communications and Networking Conference-2016 (under review)